Complexes of a-pyridone with divalent transition metals
by Clifford Carlton Houk

A thesis submitted to the Graduate Faculty in partial fulfillment of the requirements for the degree of
DOCTOR OF PHILOSOPHY in Chemistry
Montana State University

Abstract:
Six new compounds of α-pyridone (C5H5NO) have been prepared. Single crystal x-ray diffraction analysis has shown one of these compounds, CuC12.C5H5NO, to be a chlorine bridged dimer. X-ray powder diffraction data show that three of these compounds, MnC12 • 1C5H5NO, NiC12 • 1C5H5NO and CoC12 • 1C5H5NO are isomorphous and appear to have structures similar to CuC12 • 1C5H5NO. Magnetic moment, solid and solution spectrophotometric data collectively indicate that all four compounds probably have a distorted tetrahedral configuration in the solid state. C0C12 • 3 C5H5NO has been prepared; magnetic, solid and solution spectrophotometric data support an octahedral structure for this compound. The sixth compound, CuCl2 • 2 C5H5NO has not been assigned a specific structure;, the data for this compound are inconclusive

COMPLEXES OF α-PYRIDONE WITH DIVALENT TRANSITION METALS

by

CLIFFORD CARLTON HOUK

A thesis submitted to the Graduate Faculty in partial fulfillment of the requirements for the degree

of

DOCTOR OF PHILOSOPHY

in

Chemistry

Approved:

E. E. Graham
Head, Major Department

Kenneth Emerson
Chairman, Examining Committee

Louis D. Smith
Dean, Graduate Division

MONTANA STATE UNIVERSITY
Bozeman, Montana

June, 1966

ACKNOWLEDGEMENT

The author wishes to express his sincere appreciation for the advice, ever present encouragement, and continous stream of ideas given by Dr. Kenneth Emerson during the course of this study and writing of the thesis.

Appreciation is expressed to the Department of Chemistry for a graduate teaching assistantship and the Department of Health, Education and Welfare for an N.D.E.A. fellowship which made graduate study possible.

To Drs. R. J. O'Connor, William B. Cook, and K. J. Goering for their encouragement, guidance, and willingness to listen during the author's tenure at Montana State University.

To my parents, whose guidance, faith and foresightedness developed the necessary foundation upon which the building blocks of life could be securely placed.

Finally, to my wife, Evelyn, and children, Melissa and Scott, without whose confidence and encouragement none of this would have been undertaken.

TABLE OF CONTENTS

Table of Contents (Continued)

LIST OF TABLES

List of Tables (Continued)

LIST OF FIGURES

List of Figures (Continued)

List of Figures (Continued)

ABSTRACT

Six new compounds of α-pyridone (C_5H_5NO) have been prepared. Single crystal x-ray diffraction analysis has shown one of these compounds, $CuCl_2 \cdot 1\,C_5H_5NO$, to be a chlorine bridged dimer. X-ray powder diffraction data show that three of these compounds, $MnCl_2 \cdot 1\,C_5H_5NO$, $NiCl_2 \cdot 1\,C_5H_5NO$ and $CoCl_2 \cdot 1\,C_5H_5NO$ are isomorphous and appear to have structures similar to $CuCl_2 \cdot 1\,C_5H_5NO$. Magnetic moment, solid and solution spectrophotometric data collectively indicate that all four compounds probably have a distorted tetrahedral configuration in the solid state. $CoCl_2 \cdot 3\,C_5H_5NO$ has been prepared; magnetic, solid and solution spectrophotometric data support an octahedral structure for this compound. The sixth compound, $CuCl_2 \cdot 2\,C_5H_5NO$, has not been assigned a specific structure; the data for this compound are inconclusive.

INTRODUCTION

The Cu(II) ion ($3d^9$) normally has one unpaired electron in the 3d subshell. Cu(II) has a calculated spin only magnetic moment of 1.73 Bohr Magnetons (B.M.) regardless of the bond type of its compounds. Actually, the observed values of the magnetic moment are 1.9 to 2.2 B.M. for most Cu(II) compounds with ionic or weak covalent bonds and 1.72 to 1.82 B.M. for compounds with strong covalent bonds (1). Thus, Cu(II) compounds with magnetic moments lower than 1.73 B.M. are unusual. Several Cu(II) compounds with unusual magnetic moments have been prepared and investigated (Table I).

Magnetic moments are a measure of the number of unpaired electrons per atom or molecule. Paramagnetic substances contain one or more unpaired electrons per atom or molecule; diamagnetic substances have no unpaired electrons. Therefore, a subnormal magnetic moment means the number of unpaired electrons per atom or molecule has decreased; electron interaction between unpaired d electrons on closely oriented Cu atoms or unpaired d electrons with electrons from the ligand will decrease the number of unpaired electrons. Therefore, Cu(II) compounds with unusual magnetic moments must provide a pathway that permits such electron interaction.

Two possible pathways for electron interaction have been proposed; metal-metal interaction (bond formation) by direct overlap of d orbitals on closely oriented Cu atoms and a super exchange mechanism involving Cu d orbitals and $p\pi$ or $p\sigma$ orbitals of the ligand. If the first pathway were correct, one would expect the magnetic moment to be dependent upon the

Table I

Cu(II) Compounds with Subnormal Magnetic Moments

Ligand	Formula	B.M. Magnetic Moment[a]
Acetate ion	$Cu(CH_3COO)_2 \cdot 1H_2O$	1.43
Acetate ion	$Cu(CH_3COO)_2 \cdot 1C_5H_5N$	1.43
Formate ion	$Cu(HCOO)_2 \cdot 4H_2O$	1.64
Benzoate ion	$Cu(C_6H_5COO)_2 \cdot 4H_2O$	1.40
Pyridine-N-oxide	$CuCl_2 \cdot 1C_5H_5NO$	0.85
Pyridine-N-oxide	$CuCl_2 \cdot 2C_5H_5NO$	0.63
Quinoline-N-oxide	$CuCl_2 \cdot 1C_9H_7NO$	0.36
Butyrate ion	$Cu(C_3H_7COO)_2 \cdot H_2O$	1.35
Oxalate ion	$Cu(CO_2CO_2)$	1.20
Succinate ion	$Cu[CO_2(CH_2)_2CO_2]_2 \cdot 2H_2O$	1.40
N,N,Dimethylacetamide	$Cu(ClO_4)_2 \cdot [CH_3CON(CH_3)_2]_4 \cdot H_2O$	1.57
Triphenylarsine oxide	$CuBr_2 \cdot [(C_6H_2)_3AsO]_2$	1.56
1,2,4 Triazole	$CuSO_4$ 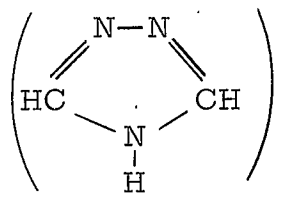 $\cdot 4H_2O$	1.62

[a]Room temperature

distance between interacting Cu atoms. If there were bond formation between Cu atoms, it would be one of three types: $\sigma(dz^2—d'z^2)$, $\pi(dxz—d'xz, dyz—d'yz)$ or $\delta(dxy—d'xy, dx^2-y^2—d'x^2-y^2)$. In a tetragonally distorted system (copper(II) acetate), π bonds are not likely because the orbitals in

question are lowest in energy of the 3d orbitals. The dx^2-y^2 level has the highest energy, but overlap between dz^2 orbitals should be greater and therefore the bonding will be determined by competition between $dz^2(\sigma)$ and $dx^2-y^2(\delta)$ orbitals. Ross and Yates (2), Ross (3) and Royer (4) favor δ bond formation. Forster and Ballhausen (5) favor σ bond formation. If a super exchange mechanism were correct, one would expect the magnetic moment to be dependent upon the electron density of the $p\pi$ and $p\sigma$ orbitals of the ligand. Schluetter (6), Kokozka (7,8) and Hansen and Ballhausen (9) state that interacting Cu atoms are only weakly coupled by d orbital overlap and suggest a super exchange pathway instead.

Super exchange was also favored in a study by Hatfield and Pascal (10) who synthesized and investigated homologs of $CuCl_2 \cdot 1C_5H_5NO$ (C_5H_5NO is pyridine-N-oxide). $CuCl_2 \cdot 1C_5H_5NO$ has been prepared and shown to be an oxygen bridged binuclear (dimeric) compound, with the structure shown in Figure 1, by Morrow, Schaefer and Smith (11). The Cu

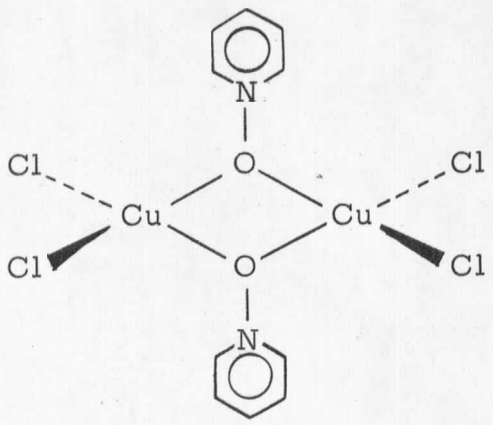

Figure 1. $CuCl_2 \cdot 1C_5H_5NO$ Structure

atoms and bridging oxygen atoms lie in the same plane; the distance between bridge Cu atoms is 3.23 ± (0.01 Å). The environment of each Cu atom is a distorted tetrahedron. Some studies listing M-M distances do not give standard deviations (uncertainties) for bond lengths. M-M distances that appear in the discussion without accompanying uncertainties may vary as much as ±0.1 Å. This compound has a magnetic moment of 0.85 B.M. at room temperature. The 3.23 Å distance between the Cu atoms makes direct d orbital interaction less likely and suggests a super exchange mechanism might be functioning. Hatfield and Pascal have substituted functional groups with different electron withdrawing and electron releasing properties in the four position of pyridine-N-oxide. The new ligands were then used to prepare a series of $CuCl_2 \cdot 1R\text{-}C_5H_4NO$ compounds (R = substituted group). They assumed the products were isostructural (oxygen bridged dimers) to $CuCl_2 \cdot 1C_5H_5NO$. The magnetic moments of their compounds decreased as the electron releasing ability of the substituent increased. The decrease of the magnetic moment indicated the electron density in the π orbitals of the bridging oxygen atoms increased and permitted increased interaction between the unpaired Cu d electrons and the oxygen π electrons. They concluded that a super-exchange mechanism was favored because the amount of overlap of the d orbitals should not be affected by ring substituents. Muto and Jonassen (12) have used mono, di and trisubstituted pyridine-N-oxides to prepare copper (II) halide complexes. Their results confirm those of Hatfield and Pascal; the magnetic moments of the compounds were dependent

upon the electron releasing ability of the substitutent. They proposed two pathways for super exchange:

1. σ path: $3d\sigma(Cu) \longleftrightarrow 2sp\sigma^2(O) \longleftrightarrow 3d\sigma(Cu)$

2. π path: $3d\pi(Cu) \longleftrightarrow 2p\pi(O) \longleftrightarrow 3d\pi(Cu)$

They suggested the σ pathway was favored from the data obtained.

Overlap of Cu d orbitals as an explanation for the sub-normal magnetic moments of some Cu(II) compounds gained support following the determination of the structure of $Cu(CH_3COO)_2 \cdot 1H_2O$ by van Niekirk and Schoening (13). The structure is shown in Figure 2. The distance between

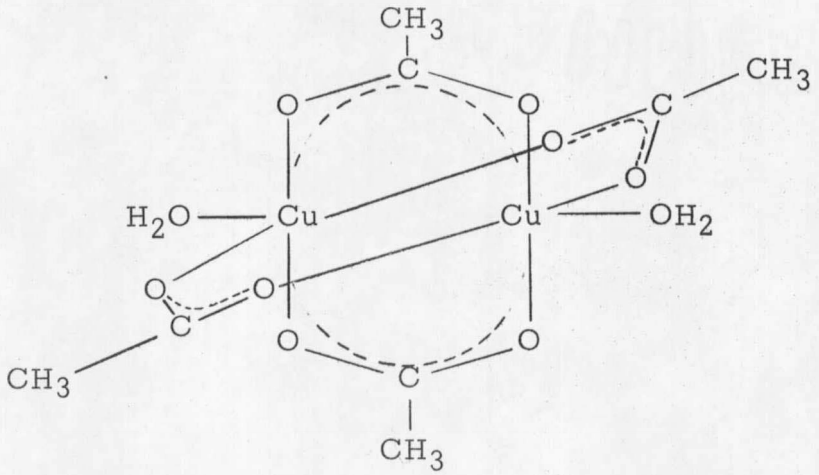

Figure 2. $Cu(CH_3COO)_2 \cdot 1H_2O$ Structure

bridged Cu atoms is 2.61 Å (14); the distance between Cu atoms in Cu metal is 2.56 ± 0.005 Å. $Cu(CH_3COO)_2 \cdot 1H_2O$ (Figure 2) has a magnetic moment of 1.43 B.M. at room temperature. The proximity of the bridged Cu atoms suggested electron interaction by overlap of d orbitals from each Cu atom.

The $Cu(CH_3COO)_2 \cdot 1\,H_2O$ results induced additional structural investigation of known Cu(II) compounds with unusual magnetic moments, particularly those containing the carboxylate group (15-21).

The carboxylate group may act as a monodentate or bidentate ligand, i.e., it may coordinate through one or both oxygen atoms. Known structures of Cu(II) carboxylate compounds with unusual magnetic moments show the carboxylate group coordinated as a bidentate ligand to two Cu atoms (binuclear) in three different configurations (Figure 3) (13, 18, 19).

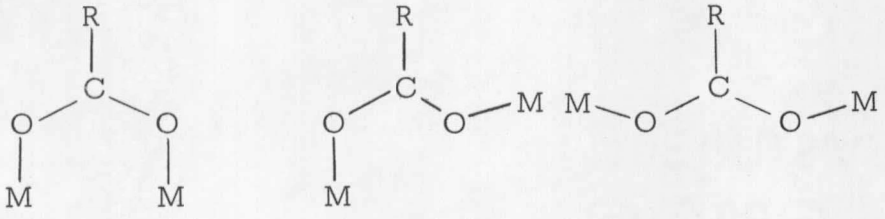

Figure 3. Observed Carboxylate Binuclear Bidentate Configurations

$Cu(CH_3COO)_2 \cdot 1\,H_2O$, therefore, has a syn-syn binuclear bidentate configuration. Other Cu(II) carboxylate compounds (structure unknown) with unusual magnetic moments are believed to be binuclear bidentate compounds.

$Cu(CH_3COO)_2 \cdot 1\,C_5H_5N$ (pyridine) has been prepared and proven isostructural (dimeric, syn-syn bidentate, bridged Cu-Cu distance 2.64 ± 0.006 Å) to $Cu(CH_3COO)_2 \cdot 1\,H_2O$ (20). $Cu(CH_3COO)_2 \cdot 1\,C_5H_5N$ has a magnetic moment of 1.43 B.M. at room temperature. Another acetate, $Cr(CH_3COO)_2 \cdot 1\,H_2O$ is also isostructural (Cr-Cr distance 2.64 Å) to

$Cu(CH_3COO)_2 \cdot 1\,H_2O$; however, $Cr(CH_3COO)_2 \cdot 1\,H_2O$ is diamagnetic at room temperature (21). Normally, Cr(II) has four unpaired electrons occupying d orbitals. The proximity of the metal ions in these compounds again suggested electron interaction through overlap of d orbitals on neighboring metal atoms.

The carboxylate group has also provided information favoring a super exchange pathway. $Cu(HCOO)_2 \cdot 4\,H_2O$ has a subnormal magnetic moment, 1.64 B.M., at room temperature (19). It has an anti-anti configuration, Figure 4 (18). The bridged Cu atoms are 5.80 ± 0.04 Å apart which precludes

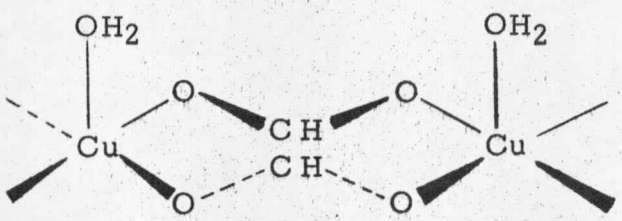

Figure 4. $Cu(HCOO)_2 \cdot 4\,H_2O$ Structure

invoking direct overlap of Cu d orbitals to explain the subnormal magnetic moment. Martin and Waterman (22) have suggested a super exchange mechanism through a π pathway of Cu $3d_{yz}$ and $3d_{xz}$ orbitals and $2p\pi$ orbitals of the bridging formate group as a possible explanation for the subnormal magnetic moment.

Several additional Cu(II) carboxylates and pyridine-N-oxide compounds have been prepared (Table I). Some have properties similar to binuclear $Cu(CH_3COO)_2 \cdot 1\,H_2O$ and $CuCl_2 \cdot 1\,C_5H_5NO$, but their structures have been unequivocally determined in only a few cases (1, 16, 23).

There are Cu(II) carboxylates (Table II) with normal magnetic moments. Other examples of Cu(II) compounds with normal magnetic moments are included.

Table II

Cu(II) Compounds with Normal Magnetic Moments

Ligand	Formula	Magnetic Moment[a] (B.M.)
Dichloroacetic acid	$Cu(Cl_2CHCOO)_2 \cdot 4H_2O$	1.74
Benzoic acid	$Cu(C_6H_5COO)_2$	1.72
o-Hydroxybenzoic acid	$Cu(HOC_6H_4COO)_2 \cdot 4H_2O$	1.92
Malonic acid	$Cu(CO_2CH_2COO) \cdot H_2O$	1.92
	$CuCl_2$	1.75
	$CuCl_2 \cdot 2H_2O$	1.87
Formic acid	$Cu(HCOO)_2$	1.75
Formic acid	$Cu(HCOO)_2 \cdot 2H_2O$	1.90
1,2,4 Triazole	$CuCl_2$ 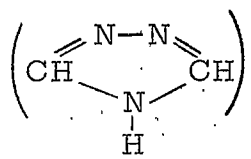	1.81

[a]Room temperature

Structural investigation of Cu(II) compounds with normal and subnormal magnetic moments, particularly the carboxylates, seem to indicate that formation of dimeric compounds and increased electron interaction is dependent upon the coordinating strengths of the ligand and solvent. The coordinating strength of the ligand, in turn, is dependent upon the electron withdrawing or releasing ability of its substituents. The exact pathway for electron interaction remains unsolved. Investigation of ligands similar to

carboxylate group or pyridine-N-oxide has been undertaken to obtain further information about the pathway.

There are ligands similar to the carboxylate group whose geometrics might permit bidentate coordination and formation of binuclear Cu(II) compounds. The acetamide group is an example, Figure 5. Other possible ligands are shown in Figure 6. Cu(II) compounds with ligands in Figures 5 and 6 might possibly increase the understanding of the electron interaction that occurs in the previously mentioned binuclear bidentate Cu(II) compounds.

Carboxylate Group Acetamido Group

Figure 5. Carboxylate and Acetamido Group Similarity

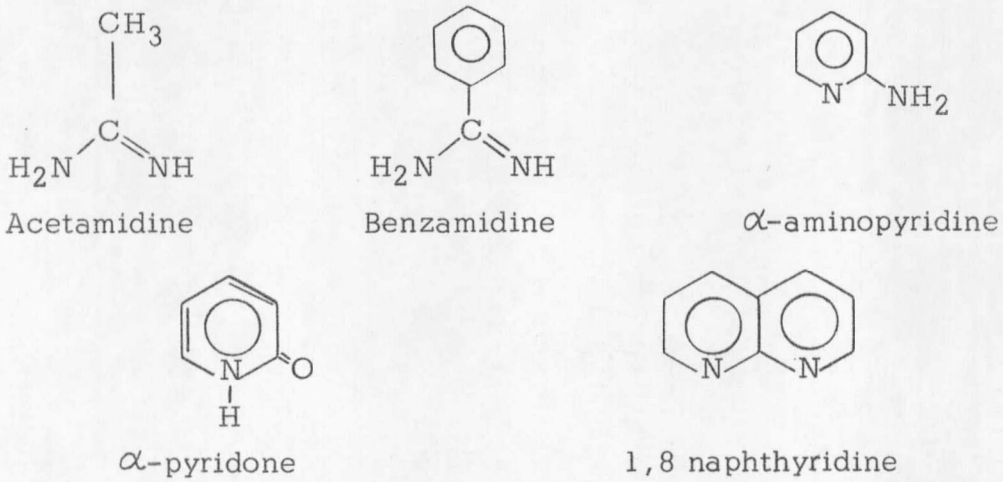

Acetamidine Benzamidine α-aminopyridine

α-pyridone 1,8 naphthyridine

Figure 6. Possible Bidentate Ligands

Synthesis and investigation of Cu(II) compounds with the acetamido group (Figure 5) was undertaken as part of a larger program. Little success was achieved with the acetamido group during two years of investigation. The results are described in Appendix A.

α-pyridone (Figure 6) is similar to the carboxylate group; it offers the possibility of bidentate coordination. It is also similar to pyridine-N-oxide, which has formed binuclear Cu(II) compounds with unusual magnetic moments. The purpose of this thesis is to report the synthesis and preliminary investigation of transition metal compounds, particularly Cu(II) and Co(II), with α-pyridone.

ANALYTICAL TECHNIQUES

This section describes the analytical techniques used in this study. The results appear in the experimental sections to follow.

Cu(II) concentrations were determined by iodometric titration as described by Kolthoff and Sandell (24). Co(II), Ni(II) and Mn(II) concentrations were found by EDTA titrations as outlined by Welcher (25). Chloride concentrations were determined by $AgNO_3$ titration with dichlorofluorescein as indicator (24). Nitrogen content was found by the macro Kjeldahl method. Triplicate samples were analyzed in all cases.

Infrared spectra were run on a Beckman IR-4 spectrophotometer between 5,000-650 cm^{-1}. The samples were prepared as micro KBr pellets. In all cases air was the reference material.

Ultraviolet and visible spectra of solutions were taken at room temperature with a Beckman DK-2 spectrophotometer equipped with 1 cm cells and standard light sources. In all cases, pure solvent was the reference material. Concentrations of 10^{-3} M and 10^{-4} M were used for visible and ultraviolet regions, respectively.

Diffuse reflectance spectra of solids were collected with a Beckman Model B spectrophotometer equipped with a diffuse reflectance attachment #12400 and a 2,000 megohm phototube resistor. The study was limited to the range 700-350 mμ by the instrument. Magnesium carbonate was used as the standard.

Magnetic susceptibilities of the powder samples were determined by the Gouy method utilizing a Mettler analytical balance, Harvey-Wells Model L-44V electromagnet and a Magnion model #HS425 power supply. The magnet was equipped with 4 inch tapered pole caps and a variable gap. The samples were suspended in a specially designed Dewar flask placed between the pole caps. The susceptibilities reported, except those of dichloro-mono-(α-pyridone) copper(II), were determined at 80°K., 210°K., 250°K. and 298°K. Liquid air was used to reach 80°K. The intermediate temperatures were obtained by placing slushes of dry ice and $CHCl_3$ (210°K) and CCl_4 (250°K) in the Dewar flask. Four field strengths were used in the study. Triplicate measurements were made at each temperature and field strength. The average of the measurements at each temperature and field strength was used to calculate gram susceptibilities from the equation:

$$\chi_g = \frac{gg'\Delta w}{dAH^2}$$

χ_g = gram susceptibility
g = Lande g factor
g' = standard gravitational constant
Δw = weight (field applied)-weight (no field)
d = sample density
A = crossectional area of Gouy tube
H = magnetic field strength

Magnetic moments were calculated from the equation:

$$\mu_{eff} = \sqrt{\frac{3\chi_m kT}{\beta^2 N}}$$

eff = magnetic moment expressed in Bohr magnetons
χ_m = χ_g times sample molecular weight
k = Boltzmann's constant
T = degrees Kelvin
β = 0.917×10^{-20}
N = Avogadro's number

To facilitate calculation of the magnetic susceptibilities and moments, a Fortran computer program was used. The computer used was the modified IBM 1620 available at the Montana State University Computing Center. Corrections for diamagnetic atoms were applied in the calculations. Magnetic field strengths were determined using $HgCo(CNS)_4$ as the standard (26).

X-ray powder diffraction data was collected with a General Electric diffractometer unit by normal crystallographic procedures. X-ray single crystal data was collected by both Weissenberg and Precession methods. Crystal parameters were calculated using standard formulae from Buerger (27).

Molecular weights were determined ebullioscopically by the Cottrell technique (98). A Beckman differential thermometer was employed in the determinations. The osmometric determinations reported were performed by Dr. W. W. Paudler of the Department of Chemistry, Ohio University, Athens, Ohio.

EXPERIMENTAL PROCEDURES AND RESULTS

Purification of α-pyridone

α-pyridone (C_5H_5NO) purchased from Aceto Chemical Company was purified by recrystallization from benzene. The crystals were white and melted at 106.5-107°C. α-pyridone was also identified spectophotmetrically and by nitrogen analysis (14.5% found, 14.7% calculated.

Figure 7 is an infrared spectrum of α-pyridone. Figures 8 to 11 represent the ultraviolet spectra of α-pyridone in H_2O, C_2H_5OH, CH_3CN and $HCON(CH_3)_2$; Table III lists the ultraviolet absorption bands and their molar absorptivities.

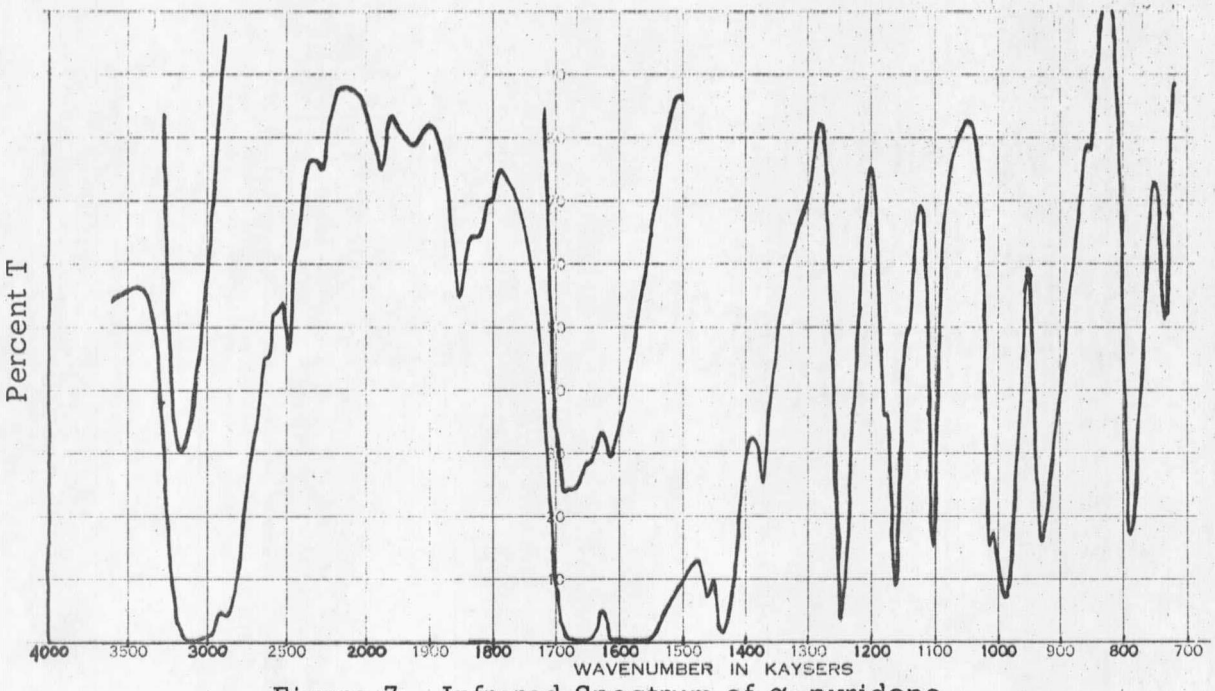

Figure 7. Infrared Spectrum of α-pyridone

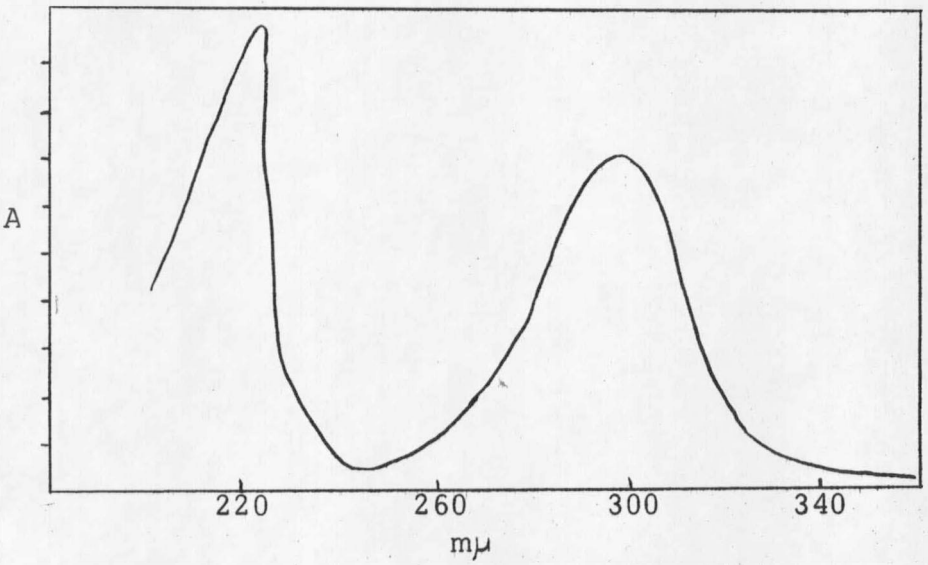

Figure 8. Ultraviolet Spectrum of α-pyridone in H_2O

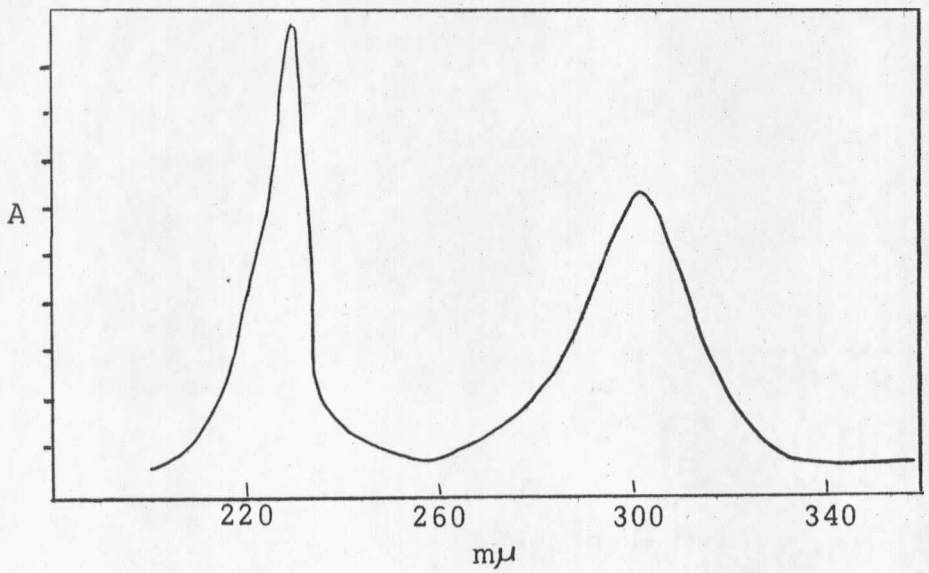

Figure 9. Ultraviolet Spectrum of α-pyridone in C_2H_5OH

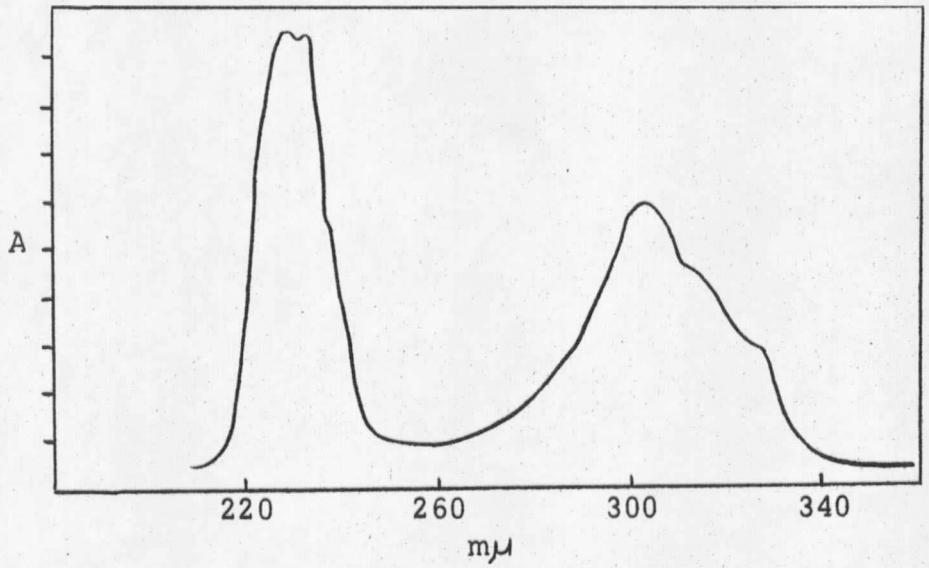

Figure 10. Ultraviolet Spectrum of α-pyridone in CH_3CN

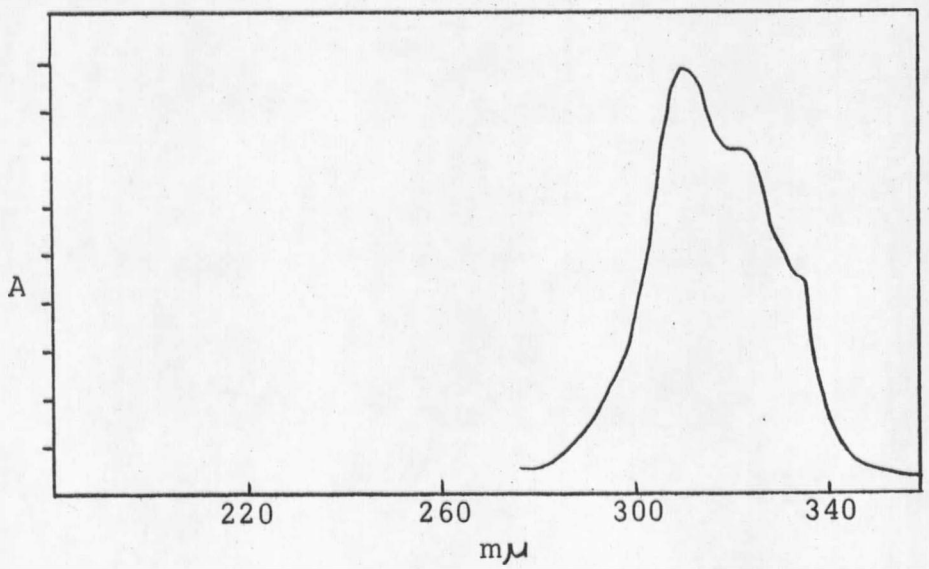

Figure 11. Ultraviolet Spectrum of α-pyridone in $HCON(CH_3)_2$

Table III

Ultraviolet Spectral Bands for α-pyridone

Solvent	Concentration	λmax(mμ)	(Molar absorptivity) ϵ max
H_2O	1.73×10^{-4} M	223	7.17×10^3
		293	5.72×10^3
C_2H_5OH	1.78×10^{-4} M	226	8.32×10^3
		298	5.23×10^3
CH_3CN	2.02×10^{-4} M	227	7.57×10^3
		229	7.53×10^3
		235(sh)[a]	-------
		302	4.85×10^3
		312(sh)	-------
		237(sh)	-------
$HCON(CH_3)_2$	1.81×10^{-4} M	305	4.80×10^3
		315(sh)	4.42×10^3
		335(sh)	-------

[a]Shoulder

Preparation of Anhydrous Metal (II) Chlorides

Anhydrous metal chlorides used throughout the study were prepared as outlined by Pray (28) from commercially available hydrates. They were stored over anhydrous $CaSO_4$ in tightly capped containers.

Solvent Purity

Solvents incorporated in the study were either MCB spectro-quality reagents or the highest purity reagent available. When water content was in doubt in alcohols, particularly CH_3OH and C_2H_5OH, they were refluxed over Mg turnings for twelve hours and then distilled. The freshly distilled alcohols were used as quickly as possible to minimize uptake of atmospheric water.

Synthesis of Dichloro-mono-α-pyridone Metal (II) Complexes

To prepare $CuCl_2 \cdot 1\,C_2H_5NO$, 1:1 molar ratios of anhydrous $CuCl_2$ and purified α-pyridone were used. The reactants were dissolved in minimum amounts of C_2H_5OH and the α-pyridone solution was added dropwise to the Cu(II) solution with stirring. Precipitation occurred after approximately one-half of the α-pyridone solution had been added. The solid produced was an orange powder; the filtrate was green. Cooling the filtrate produced more of the orange solid. Recrystallization from C_2H_5OH produced needle-like crystals. Analysis of the compound indicated the emperical molecular formula was $CuCl_2 \cdot 1\,C_5H_5NO$.

The ease with which the compound was produced prompted a literature search to determine if compounds similar to α-pyridone had been used as ligands with transition metal ions. A series of compounds, $MX_2 \cdot L_n$ (M = metal ion, X = halide, nitrate, perchlorate, L = pyridine-N-oxide (C_5H_5NO), n = 1, 2, 3, 4) had been prepared by Quagliano (29). The compounds had been synthesized and recrystallized from ethanolic solutions. A few of these compounds exhibited subnormal magnetic moments. One of the compounds with a low moment, $CuCl_2 \cdot 1\,C_5H_5NO$, had been shown to be an oxygen bridged binuclear compound (Figure 1, page 3). This compound had a magnetic moment of 0.85 B.M. Because some of the pyridine-N-oxide compounds exhibited subnormal magnetic moments and α-pyridone was structurally similar to pyridine-N-oxide, synthesis of a related series, $MX_2 \cdot L_1$ (M = transition metal, X = chloride, L = α-pyridone), was undertaken. The reactants were mixed as previously described for the synthesis of

dichloro-mono-α-pyridone copper(II). Compounds with the empirical formula $MCl_2 \cdot 1\,C_5H_5NO$ have been synthesized using Cu(II), Co(II), Ni(II) and Mn(II) chlorides and recrystallized from C_2H_5OH. Table IV lists the results of elemental analyses performed as described in the analytical section.

Table IV

$MCl_2 \cdot 1\,C_5H_5NO$ Elemental Analyses

Metal		% M	% Cl^-	% N	Color	Nature
Cu(II)	Found	27.7±0.23	30.9±0.23	5.8±0.17	orange	needle-like
	Calc.	27.7	30.9	6.1		crystals
Co(II)		26.0±0.40	31.5±0.17	6.4±0.41	blue-	needle-like
		26.2	31.6	6.2	violet	crystals
Ni(II)		25.8±0.17	31.0±0.00	6.4±0.33	salmon	powder
		26.1	31.6	6.2		
Mn(II)		24.3±0.75	31.0±0.17	6.5±0.28	off-white	powder
		24.9	32.1	6.3		

Magnetic susceptibilities and moments, calculated as described in the analytical section, are listed in Table V.

Table VI indicates d spacings and θ angles of the six most intense powder diffraction lines, obtained with the General Electric diffractometer, for each of the complexes. The d values were calculated from the equation;

$$n\lambda = 2\,d \sin\theta$$

where
- $n = 1$
- λ = wavelength of incident radiation
- d = distance between layers
- θ = diffraction angle

Table V

$MCl_2 \cdot 1\,C_5H_5NO$ Magnetic Susceptibilities and Moments

Metal	Temp. °K	χ_m(cgs, esu) x 10^6 Magnetic Susceptibility	(B.M.) Magnetic Moment
Cu(II)	80°	6,970	2.13
	298°	1,540	1.93
Co(II)	80°	53,300	5.91
	210°	21,100	6.03
	250°	17,000	5.90
	298°	11,900	5.39
Ni(II)	80°	31,800	4.57
	210°	8,600	3.86
	250°	7,000	3.80
	298°	5,400	3.65
Mn(II)	80°	52,400	5.86
	210°	19,800	5.83
	250°	17,700	6.03
	298°	14,600	5.97

Table VI

$MCl_2 \cdot 1\,C_5H_5NO$ Powder Diffraction Data

Cu(II)			Co(II)			Ni(II)			Mn(II)		
θ	d	Rel. Int.	θ	d	Rel. Int.	θ	d	Rel. Int.	θ	d	Rel. Int.
3.9	11.3	100	3.9	11.3	100	3.8	11.6	100*	3.9	11.3	100*
5.0	8.8	70	4.8	9.2	85	4.7	9.4	75	4.8	9.2	80
7.5	5.9	75	5.9	7.5	70	5.8	7.6	65	5.8	7.6	60
9.1	4.9	25	7.3	6.1	90	7.2	6.2	70	7.2	6.2	90
10.9	4.1	25	8.9	5.0	70	8.9	5.0	40	8.9	5.0	90
14.4	3.1	50	14.8	3.0	60	14.9	3.0	70	14.6	3.1	75

*Very intense

Single crystal x-ray diffraction data show the Cu(II) complex is triclinic with space group PT. Its cell dimensions are: a = 9.93 Å, b = 9.94 Å, c = 3.95 Å with α = 90.9°, β = 92.9° and γ - 113.2°. There are two formula units per unit cell. The cobalt complex is monoclinic and of space group $C2_1/C$. Its cell dimensions are; a = 24.8 Å, b = 16.7 Å, c = 8.7 Å with γ = 94°. There are 16 formula units per unit cell.

The ultraviolet spectra of the $MCl_2 \cdot 1C_5H_5NO$ complexes are essentially identical to those of α-pyridone previously shown in Figures 8 to 11, pages 15 and 16. The complexes, in general, exhibit lower molar absorptivities than free α-pyridone. Table VII lists the ultra-violet absorption bands and molar absorptivities of the complexes.

Table VII

$MCl_2 \cdot 1C_5H_5NO$ Ultraviolet Absorption Bands and Molar Absorptivities

Solvent	Cu(II) (mμ) λ max	∈ max	Co(II) (mμ) λ max	∈ max	Ni(II) (mμ) λ max	∈max	Mn(II) (mμ) λ max	∈max
H_2O	223	6900	222	7700	223	8080	223	8450
	292	6130	294	6420	291	6480	230(sh)	
							294(sh)	6750
							315(sh)	
C_2H_5OH	226	7420	227	8480	227	8530	226	8530
	298	6220	298	5280	298	5580	298	5760
CH_3CN	223(sh)		226	9430				
	226	9330	229(sh)					
	234(sh)		233(sh)					
	257	2670	257	2870				
	305	5290	302	5330				
	310(sh)		312(sh)					
	328(sh)		328(sh)					
$HCON(CH_3)_2$					305	5280	305	11600
					315(sh)		315(sh)	
					330(sh)		332(sh)	

Visible spectra for these complexes are shown in Figures 12-20. Their absorption bands and molar absorptivities are listed in Table VIII.

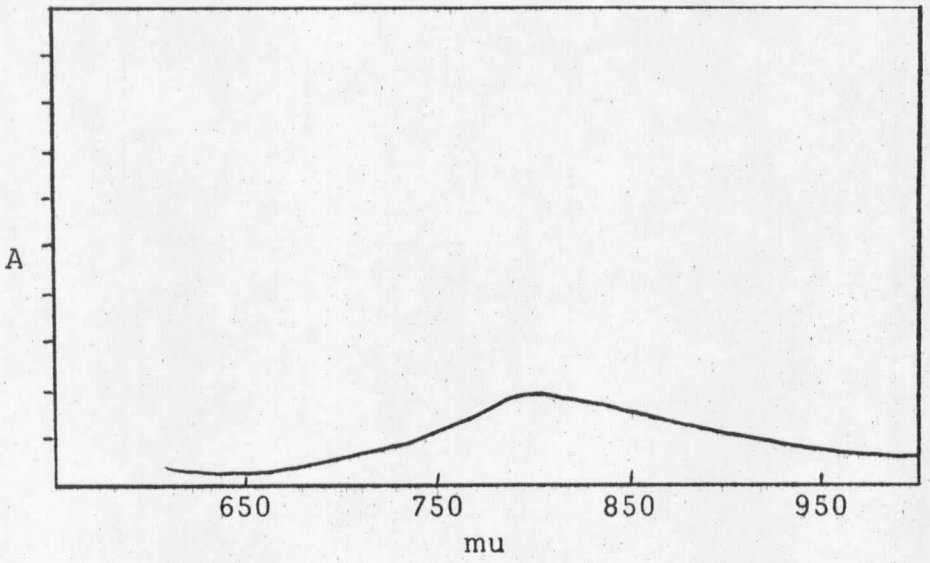

Figure 12. Visible Spectrum of $CuCl_2 \cdot 1\,C_5H_5NO$ in H_2O

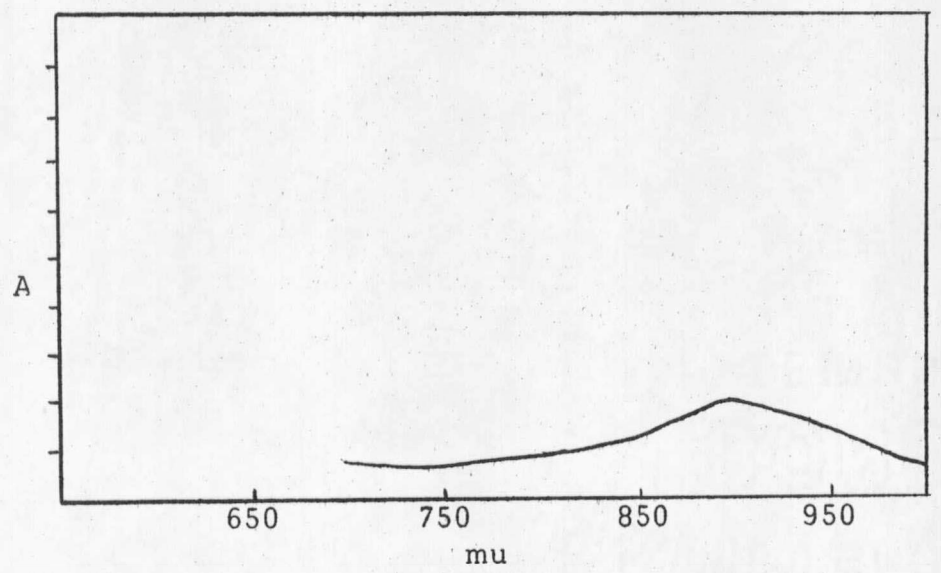

Figure 13. Visible Spectrum of $CuCl_2 \cdot 1\,C_5H_5NO$ in C_2H_5OH

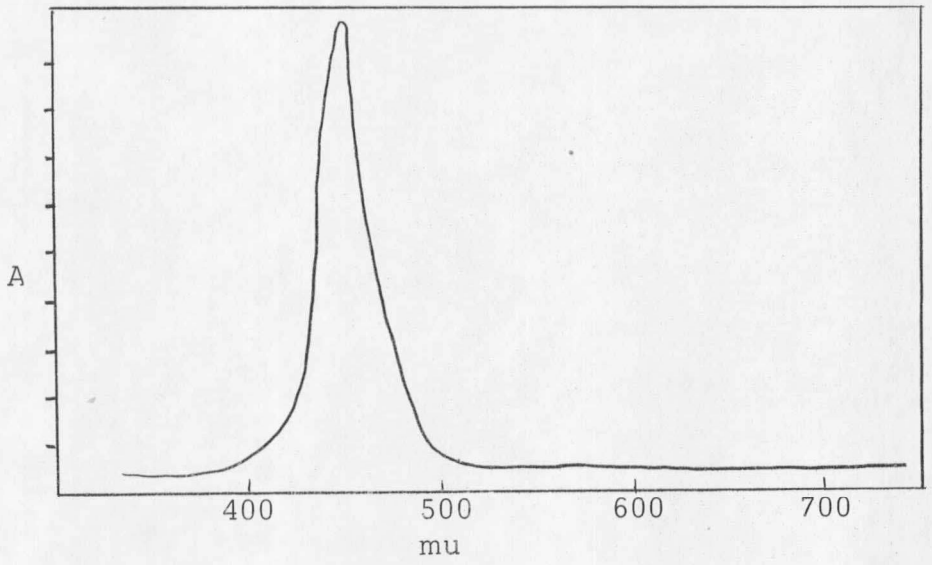

Figure 14. Visible Spectrum of $CuCl_2 \cdot 1\,C_5H_5NO$ in CH_3CN

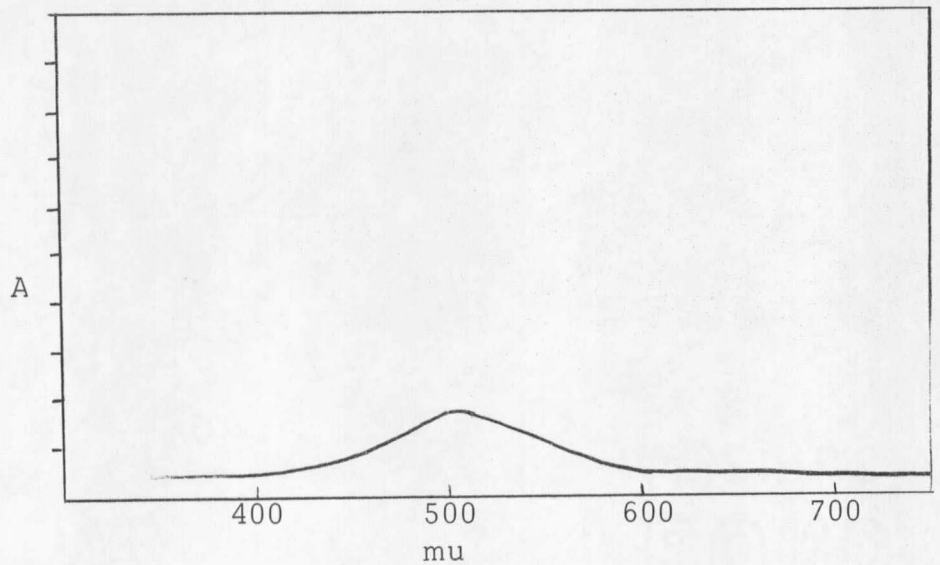

Figure 15. Visible Absorption Spectrum of $CoCl_2 \cdot 1\,C_5H_5NO$ in H_2O

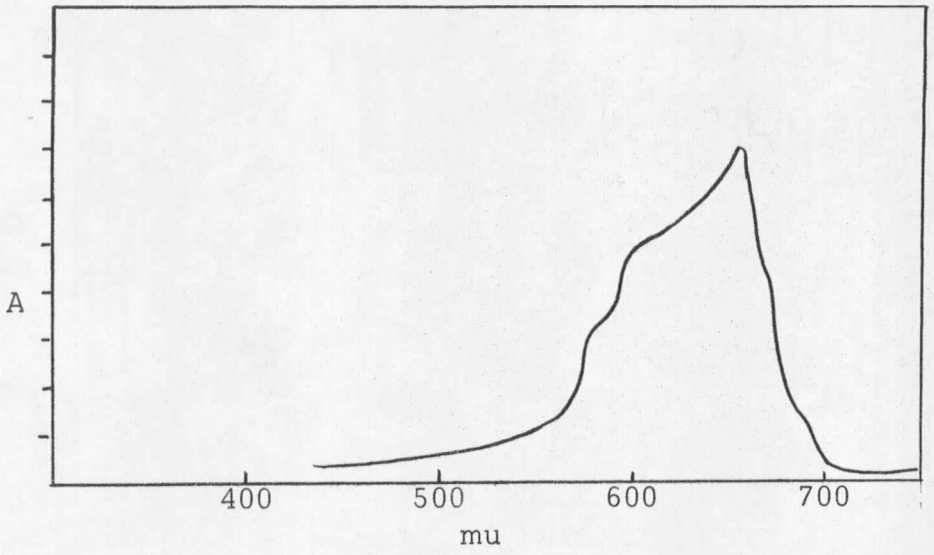

Figure 16. Visible Absorption Spectrum of $CoCl_2 \cdot 1\,C_5H_5NO$ in C_2H_5OH

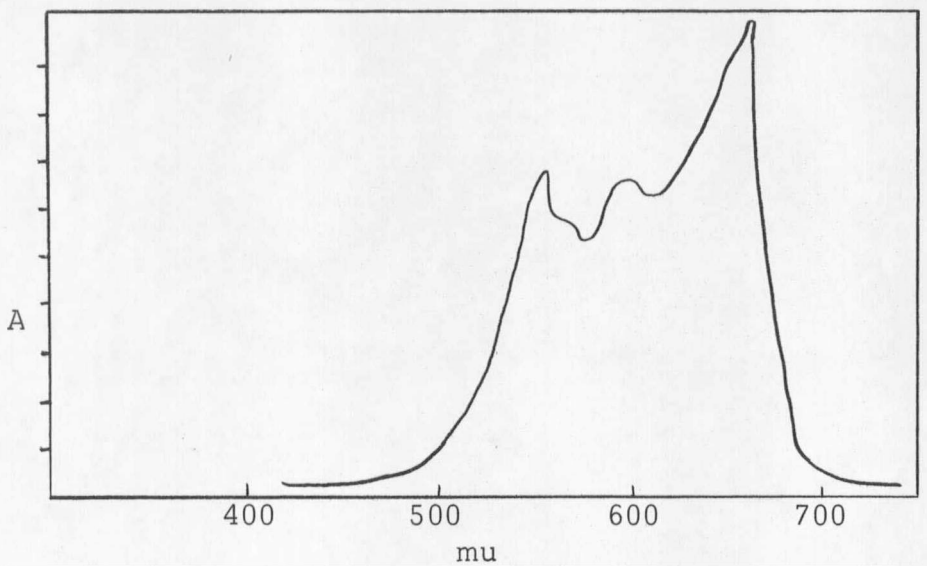

Figure 17. Visible Absorption Spectrum of $CoCl_2 \cdot 1\,C_5H_5NO$ in HC_3CN

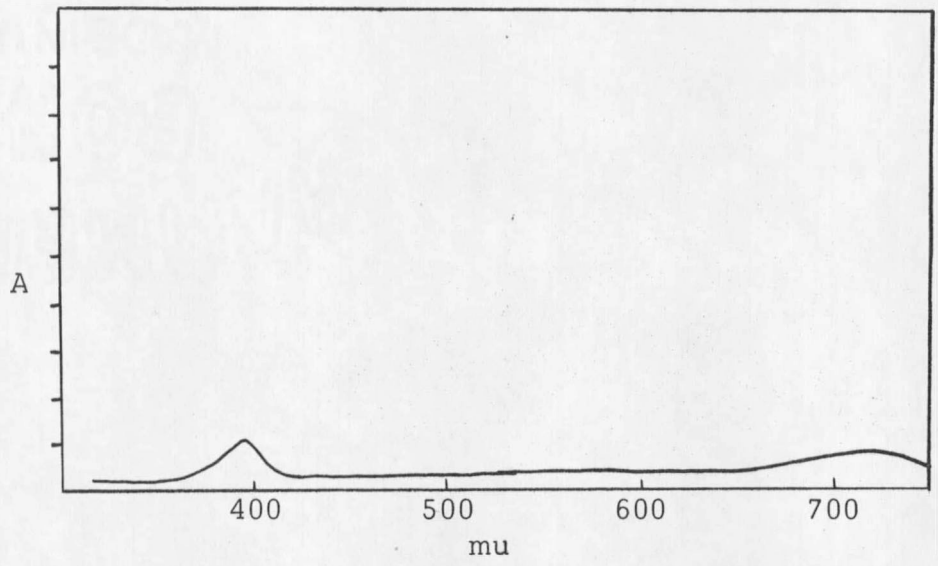

Figure 18. Visible Absorption Spectrum of $NiCl_2 \cdot 1\,C_5H_5NO$ in H_2O

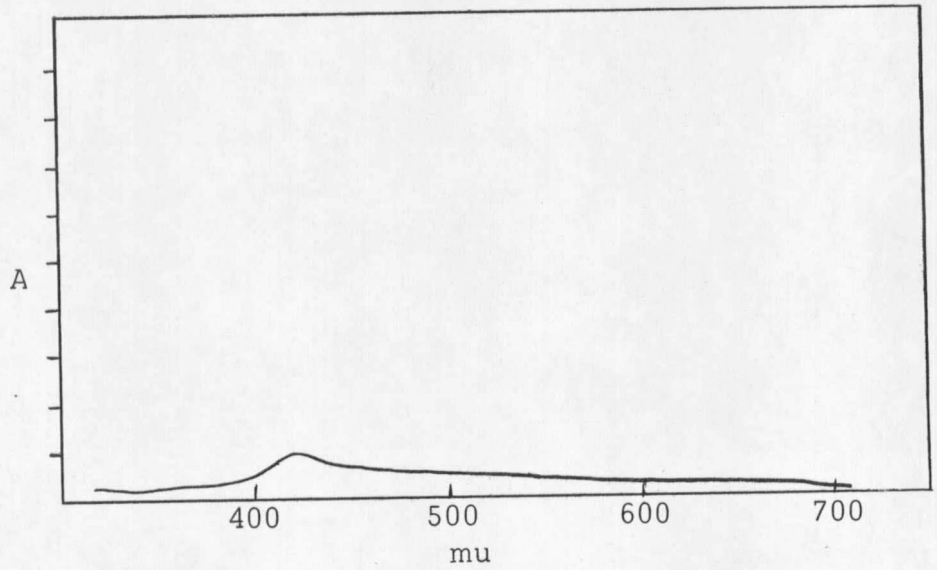

Figure 19. Visible Absorption Spectrum of $NiCl_2 \cdot 1\,C_5H_5NO$ in C_2H_5OH

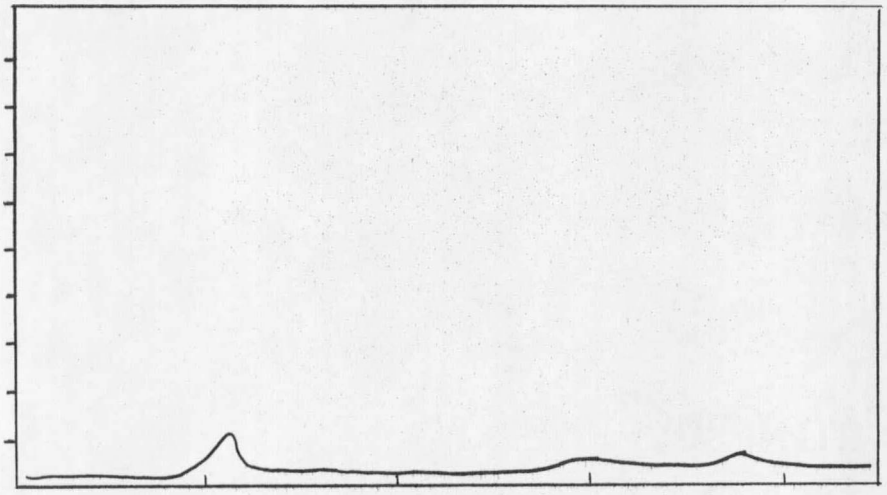

Figure 20. Visible Absorption Spectrum of $NiCl_2 \cdot 1\,C_5H_5NO$ in $HCON(CH_3)_2$

Table VIII

$MCl_2 \cdot 1\,C_5H_5NO$ Visible Band Spectra and Molar Absorptivities

	Cu(II)		Co(II)		Ni(II)	
Solvent	λ max (mu)	∈max	λ max (mu)	∈max	λ max (mu)	∈max
H_2O	790	128	498	5.1	385	6.2
					700(v.b.)	2.5
C_2H_5OH	880	164	575(sh)		413	10.7
			612(sh)			
			638	168.0		
			655(sh)			
			665(sh)			
CH_3CN	450	931	556	258.0		
			570(sh)			
			590	266.0		
			610(sh)			
			650(sh)			
			660	402.0		
$HCON(CH_3)_2$					410	51.00
					575(sh)	46.0
					602	28.0

Diffuse reflectance spectra for the complexes are shown in Figures 21-24.

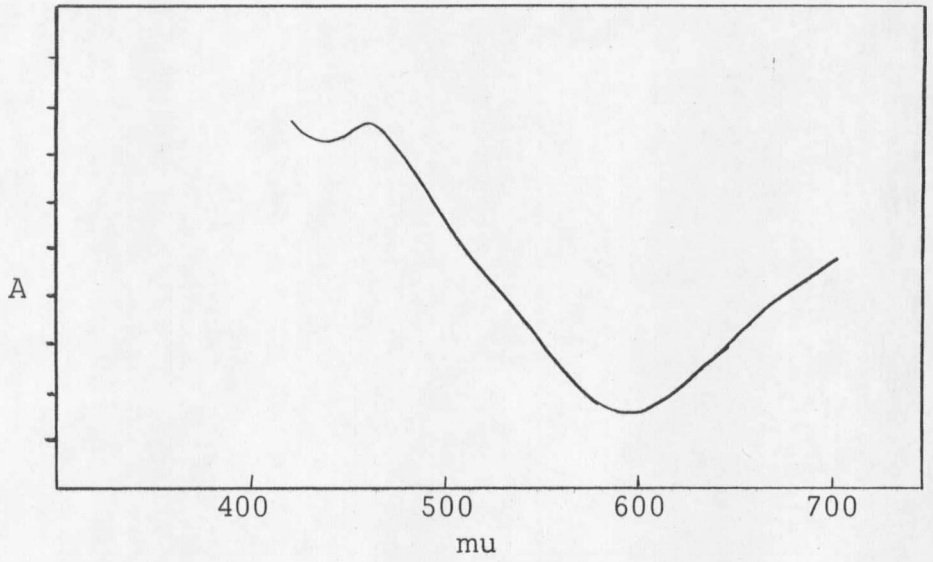

Figure 21. Diffuse Reflectance Spectrum of $CuCl_2 \cdot 1C_5H_5NO$

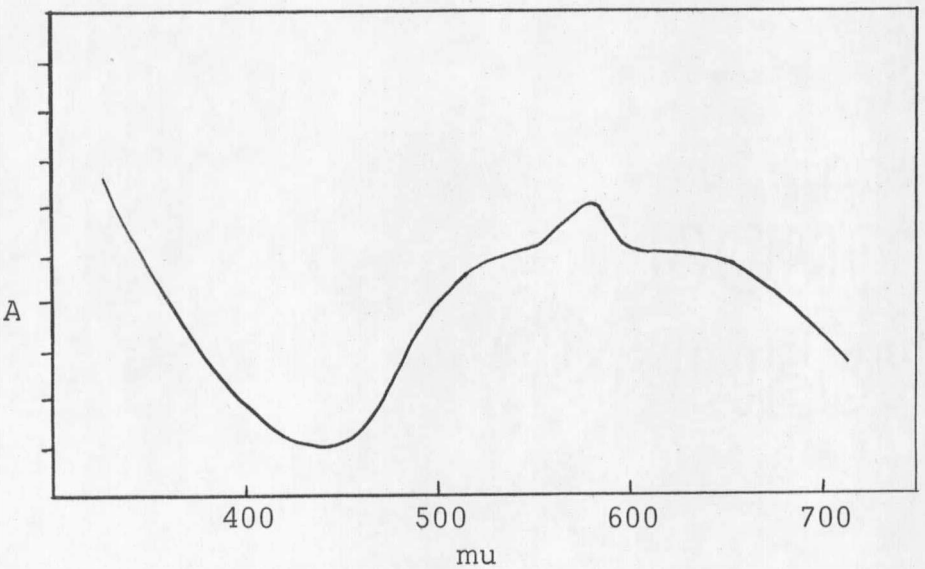

Figure 22. Diffuse Reflectance Spectrum of $CoCl_2 \cdot 1C_5H_5NO$

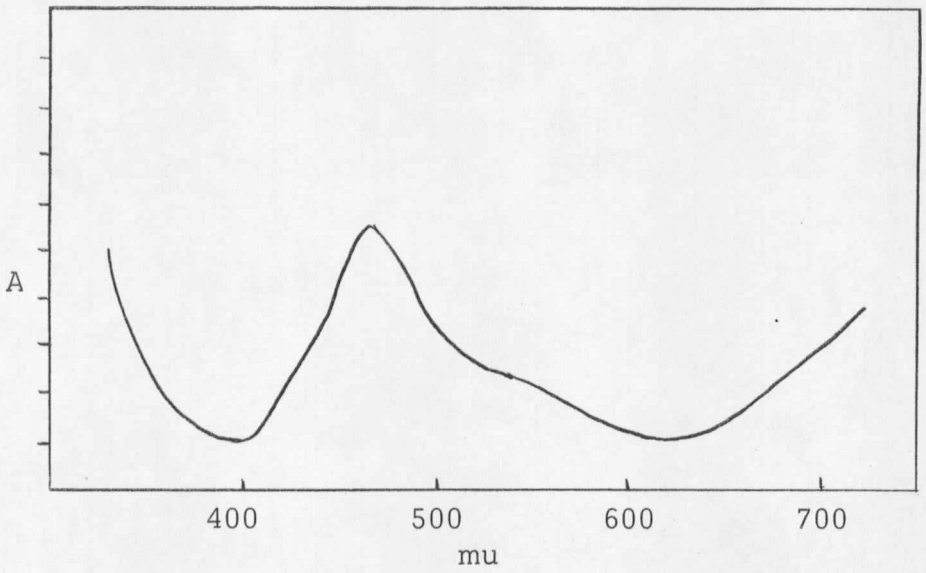

Figure 23. Diffuse Reflectance Spectrum of $NiCl_2 \cdot 1\,C_5H_5NO$

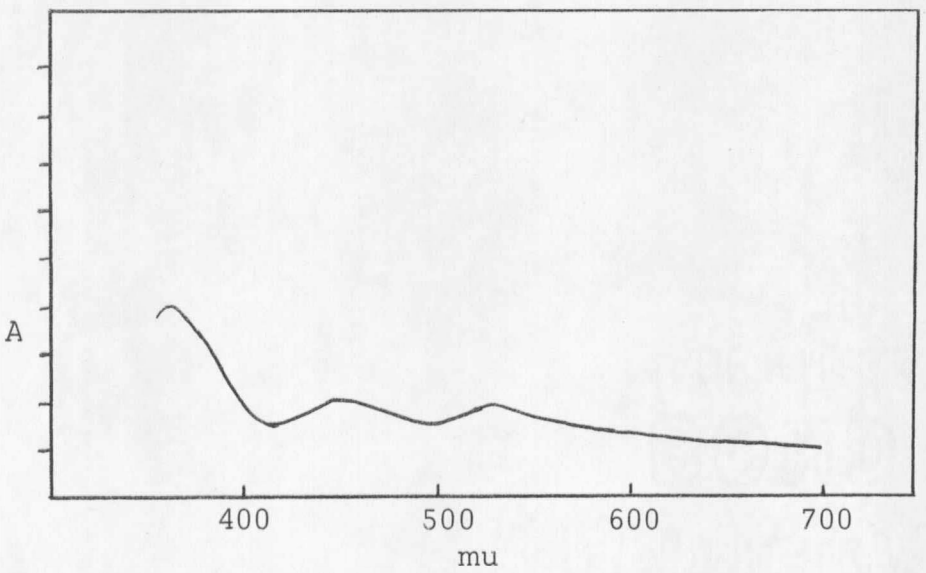

Figure 24. Diffuse Reflectance Spectrum of $MnCl_2 \cdot 1\,C_5H_5NO$

Infrared spectra of the complexes also resemble the spectrum of α-pyridone. Some characteristic absorption bands used for interpretation exhibit shifts in frequency and intensity. The infrared spectra of the complexes are shown in Figures 25-28. Band assignments and interpretation of the observed shifts appear in the discussion section of the thesis.

Molecular weight determinations were performed as previously described for all but the Mn(II) complex. The results are listed in Table IX.

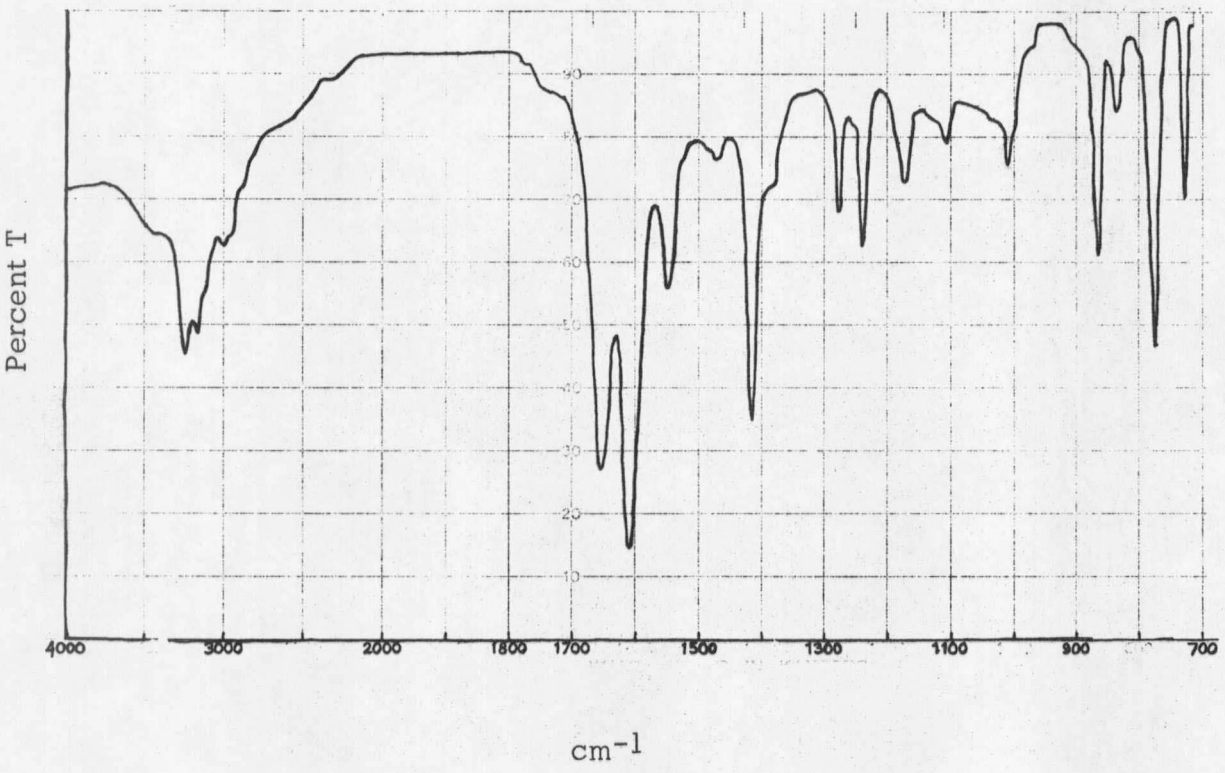

Figure 25. Infrared Spectrum of $CuCl_2 \cdot 1\,C_5H_5NO$

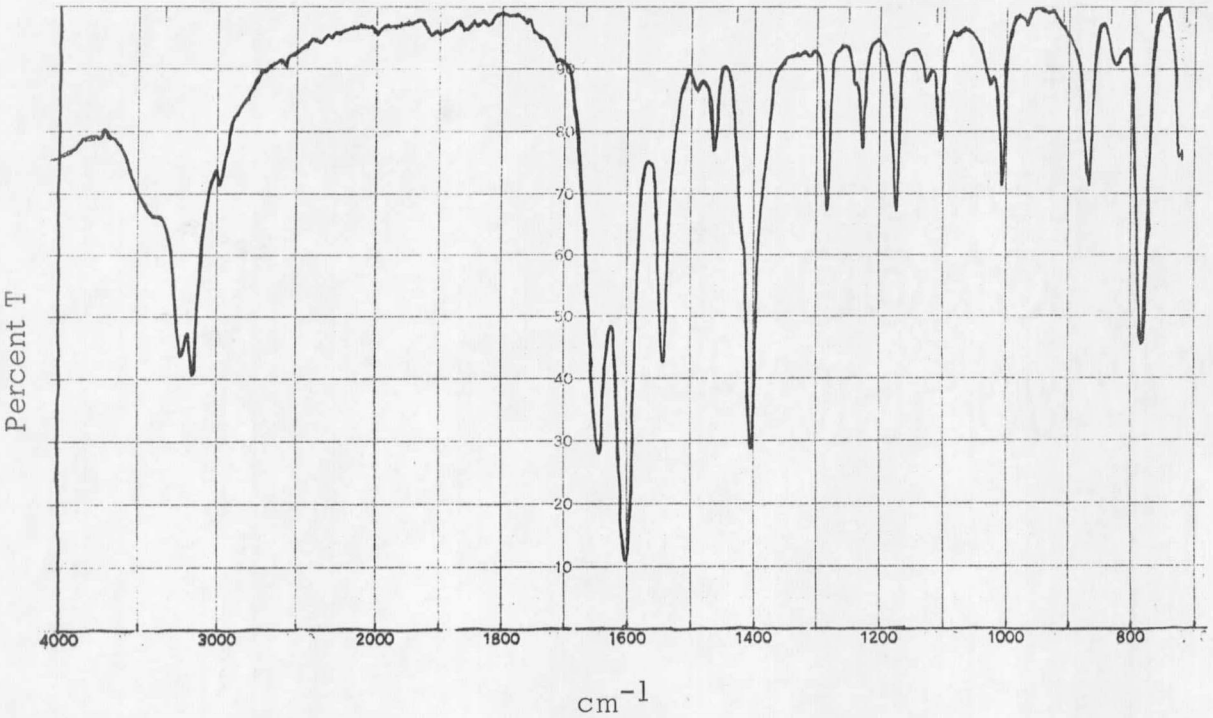

Figure 26. Infrared Spectrum of $CoCl_2 \cdot 1\,C_5H_5NO$

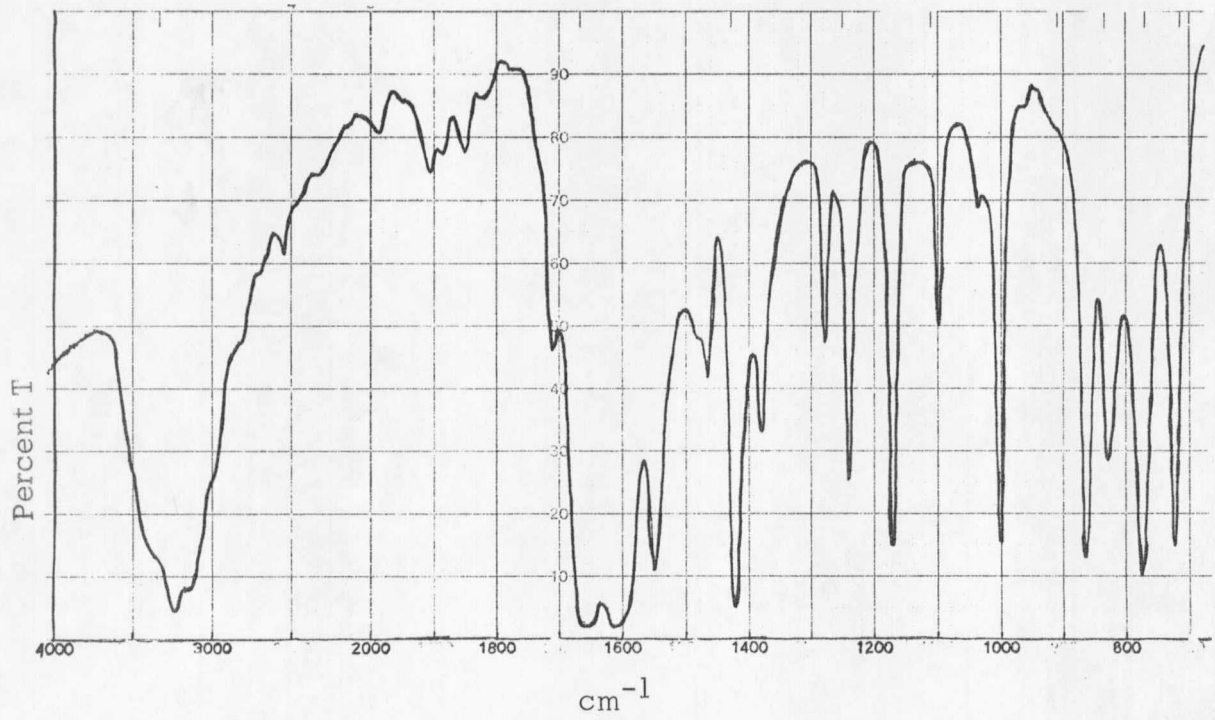

Figure 27. Infrared Spectrum of $NiCl_2 \cdot 1\,C_5H_5NO$

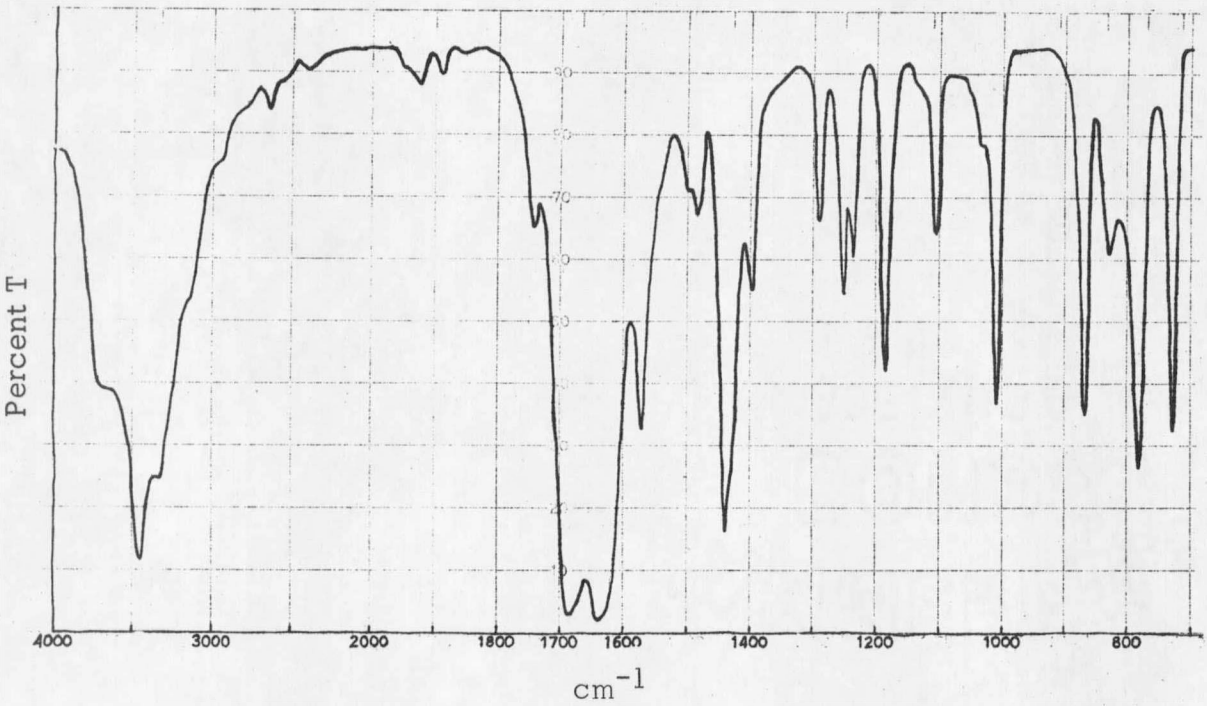

Figure 28. Infrared Spectrum of $MnCl_2 \cdot 1\,C_5H_5NO$

Table IX

$MCl_2 \cdot 1\,C_5H_5NO$ Molecular Weight by Determinations

Compound	Solvent	Method	Found	Empirical Mole. Wt.[a]
$CuCl_2 \cdot 1\,C_5H_5NO$	CH_3CN	Ebullioscopic	865	230
	C_2H_5OH	Osmometric[b]	975	230
	$HCON(CH_3)_2$	Ebullioscopic	84	230
$CuCl_2$	$HCON(CH_3)_2$	Ebullioscopic	135	135
$CoCl_2 \cdot 1\,C_5H_5$	C_2H_5OH	Ebullioscopic	118	225
	C_2H_5OH	Osmometric	1,195	225
	C_2H_5OH	Osmometric	1,079	225
	$HCON(CH_3)_2$	Ebullioscopic	115	225
$NiCl_2 \cdot 1\,C_5H_5$	$HCON(CH_3)_2$	Ebullioscopic	40	225

[a] Theoretical monomer molecular weight

[b] Determined by Dr. W. W. Paudler, Department of Chemistry, Ohio University

Synthesis of Dichloro-n-α-pyridone Metal (II) Complexes

Quagliano had also prepared $CuCl_2 \cdot 2\,C_5H_5NO$ (pyridine-N-oxide), a chartreuse powder, and blue $CoCl_2 \cdot 3\,C_5H_5NO$ (pyridine-N-oxide). Syntheses in which arbitrary Cu(II): α-pyridone molar ratios were used, prior to synthesis of mono-α-pyridone complexes, had produced a chartreuse powder whose elemental analyses (19.5% Cu, 21.7% Cl, 9.3% N) were close to the calculated values of $CuCl_2 \cdot 2\,C_5H_5NO$ (α-pyridone). Therefore, 1 copper(II): 2 α-pyridone molar ratios (ethanolic solutions) were mixed as before (dropwise, page 18) and a chartreuse powder precipitated, after approximately one-half of the Cu(II) had been added. One cobalt(II):3 α-pyridone ethanolic solutions were reacted in the same manner and a blue crystalline solid precipitated. All of the previously described methods of identification were performed on these complexes except molecular weight determinations. The results of these methods for both complexes have been combined for presentation. Elemental analyses appear in Table X.

Table X

$CuCl_2 \cdot 2\,C_5H_5NO$ and $CoCl_2 \cdot 3\,C_5H_5NO$ Elemental Analyses

	% M	% Cl^-	% N	Color	Nature
Cu Found	20.0±0.17	22.2±0.28	8.65±0.16	chartreuse	powder
Calc.	19.6	21.9	8.63		
Co Found	14.6±0.00	17.65±0.06	9.8±0.33	blue	crystalline
Cal.	14.2	17.1	10.1		

X-ray powder data for the six most intense powder diffraction lines appear in Table XI.

Table XI

$CuCl_2 \cdot 2\,C_5H_5NO$ and $CoCl_2 \cdot 3\,C_5H_5NO$ Powder Diffraction Data

Cu(II)			Co(II)		
θ	3	Rel. Int.	θ	d	Rel. Int.
4.2	10.5	90	6.1	7.25	90
5.0	8.84	95	8.2	5.40	70
5.8	7.62	100	8.3	5.34	70
7.1	6.23	95	9.2	4.82	100
9.6	4.62	80	13.4	3.33	60
10.0	4.44	85	15.2	2.94	55

Again the ultraviolet spectra resemble those of α-pyridone. The absorption bands and molecular absorptivities are listed in Table XII.

Table XII

$CuCl_2 \cdot 2$ α-pyridone and $CoCl_2 \cdot 3$ α-pyridone U.V. Spectral Bands

Complex	Solvent	Concentration	(mμ) λmax	(molar absorptivity) ∈max
$CuCl_2 \cdot 2\alpha$	H_2O	2.11×10^{-5}M	223	1.52×10^4
			293	1.33×10^4
	CH_3CN	1.06×10^{-5}M	225(sh)[a]	
			230(sh)	
			234(sh)	
			303	1.13×10^4
			315(sh)	
			330(sh)	
$CoCl_2 \cdot 3\alpha$	H_2O	4.08×10^{-6}M	223	2.71×10^4
			295	2.21×10^4
	C_2H_5OH	4.28×10^{-6}M	225	2.33×10^4
			305	1.48×10^4
	CH_3CN	4.53×10^{-6}M	230(sh)	
			235(sh)	
			303	1.76×10^4
			315(sh)	
			330(sh)	

[a]Shoulder

Figure 29-33 are the visible spectra of the complexes and Table XIII lists the absorption bands and their molar absorptivities.

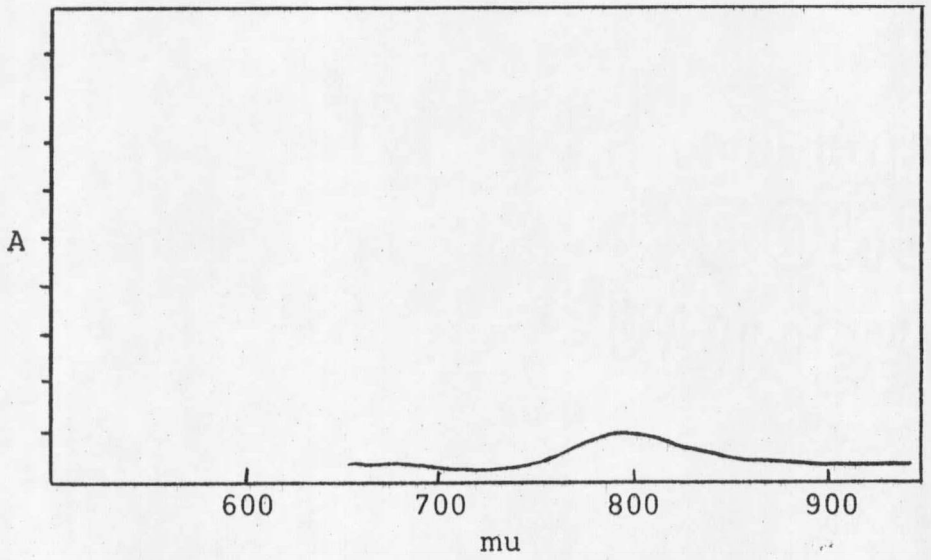

Figure 29. Visible Absorption Spectrum of $CuCl_2 \cdot 2\,C_5H_5NO$ in H_2O

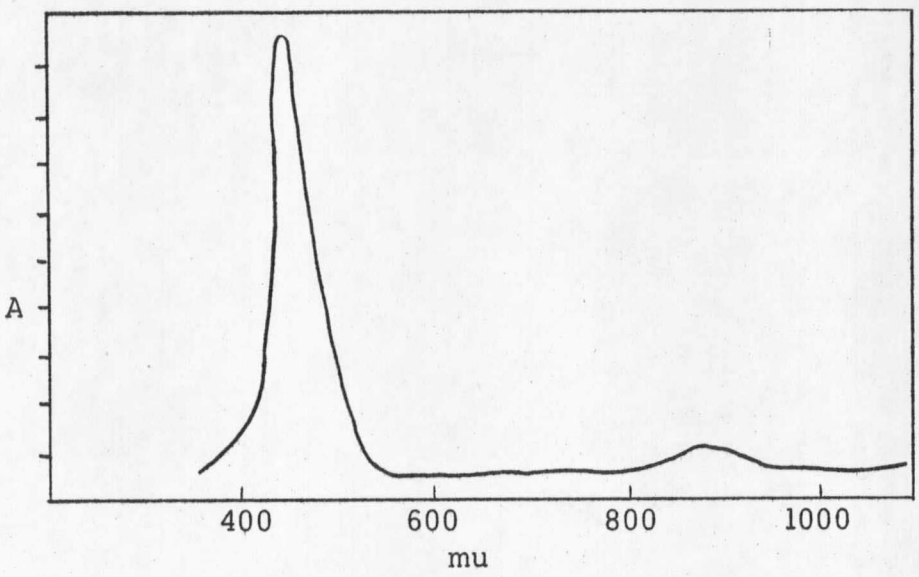

Figure 30. Visible Absorption Spectrum of $CuCl_2 \cdot 2\,C_5H_5NO$ in CH_3CN

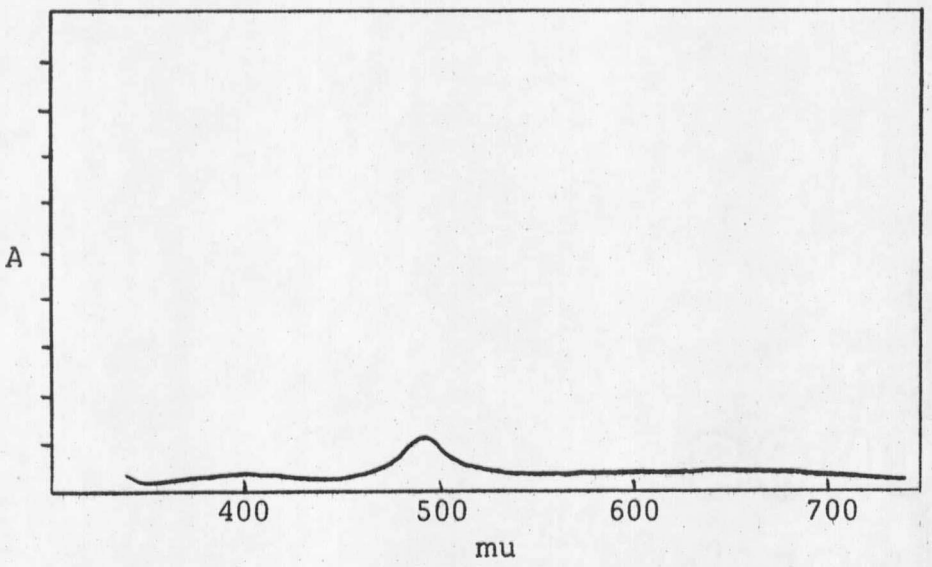

Figure 31. Visible Absorption Spectrum of $CoCl_2 \cdot 3C_5H_5NO$ in H_2O

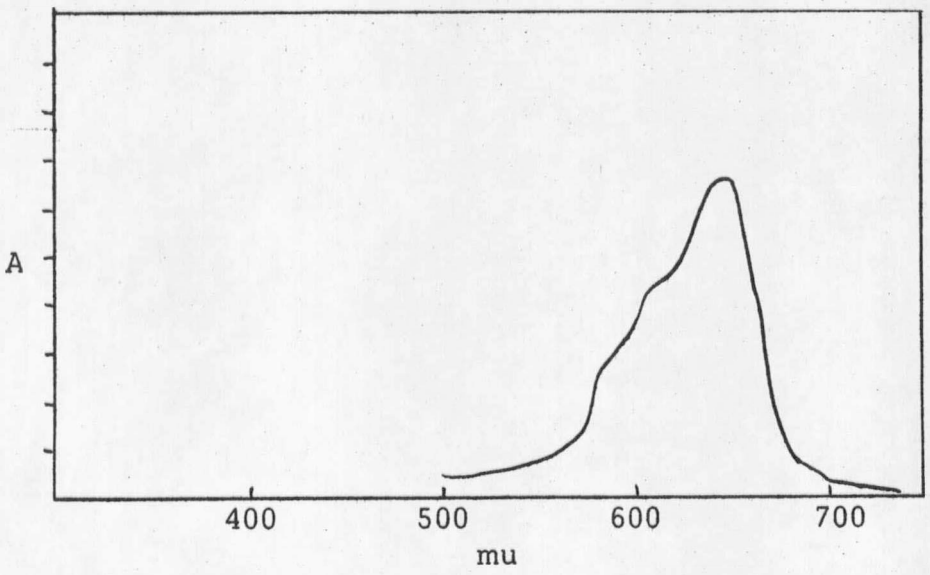

Figure 32. Visible Absorption Spectrum of $CoCl_2 \cdot 3C_5H_5NO$ in C_2H_5OH

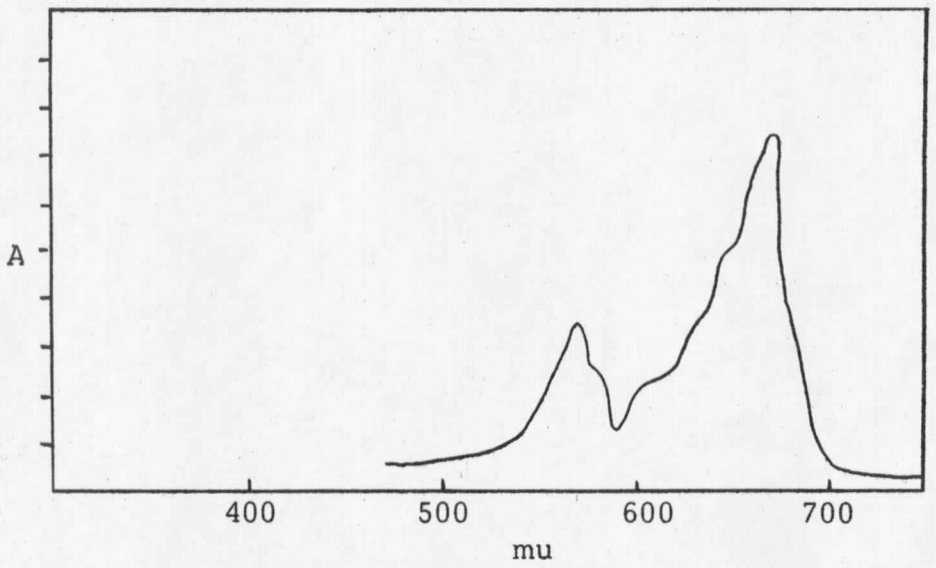

Figure 33. Visible Absorption Spectrum of $CoCl_2 \cdot 3\,C_5H_5NO$ in CH_3CN

Table XIII

$CuCl_2 \cdot 2\,C_5H_5NO$ and $CoCl_2 \cdot 3\,C_5H_5NO$ Visible Absorption Bands

Complex	Solvent	Conc.	(mu) λ max	(molar absorptivity) ϵ max
$CuCl_2 \cdot 2\,C_5H_5NO$	H_2O	5.28×10^{-3}M	786(v.b.)[a]	13
	CH_3CN	1.06×10^{-3}M	875(v.b.)	75
			450	775
$CoCl_2 \cdot 3\,C_5H_5NO$	H_2O	4.08×10^{-3}M	490	7
	C_2H_5OH	4.28×10^{-3}M	575(sh)	
			600(sh)	
			640	152
	CH_3CN	4.53×10^{-3}M	565	97
			575(sh)	
			600(sh)	
			613(sh)	
			660	159

[a]Very broad

Figures 34 and 35 are the diffuse reflectance spectra of the complexes.

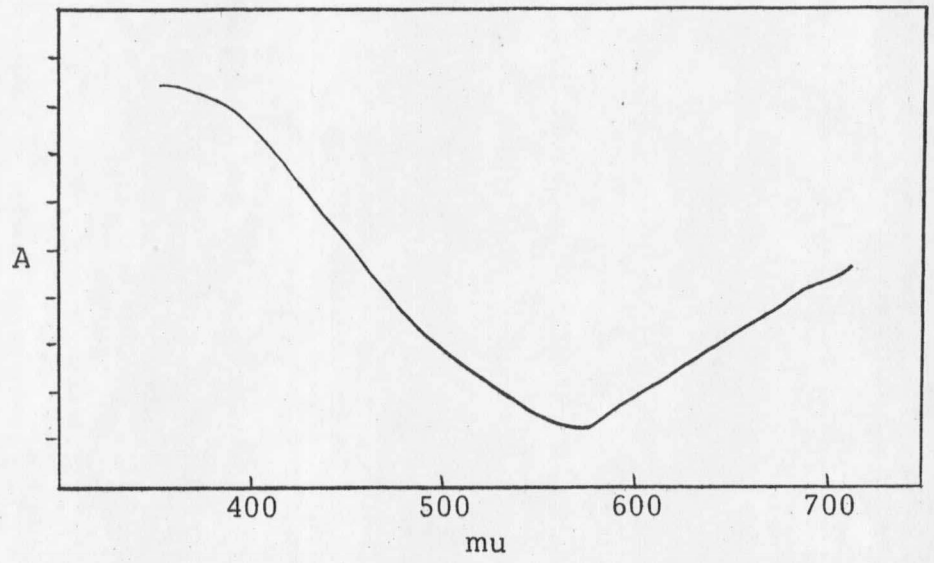

Figure 34. Diffuse Reflectance Spectrum of $CuCl_2 \cdot 2\,C_5H_5NO$

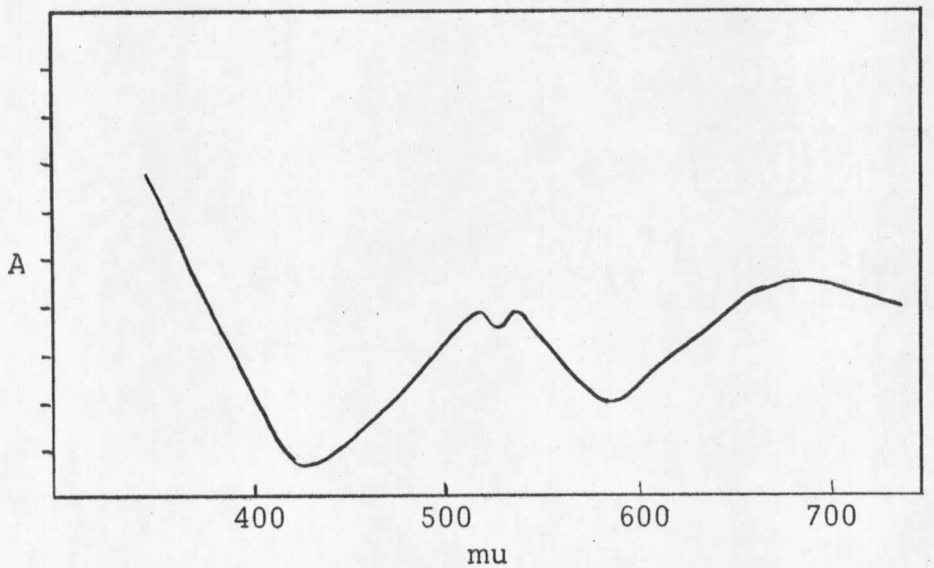

Figure 35. Diffuse Reflectance Spectrum of $CoCl_2 \cdot 3\,C_5H_5NO$

The infrared spectra of these complexes also resemble the α-pyridone spectrum with differences similar to the mono-α-pyridone complexes. The spectra appear in Figures 36 and 37. Band assignments and interpretation of the observed shifts again appear in the discussion section of the thesis.

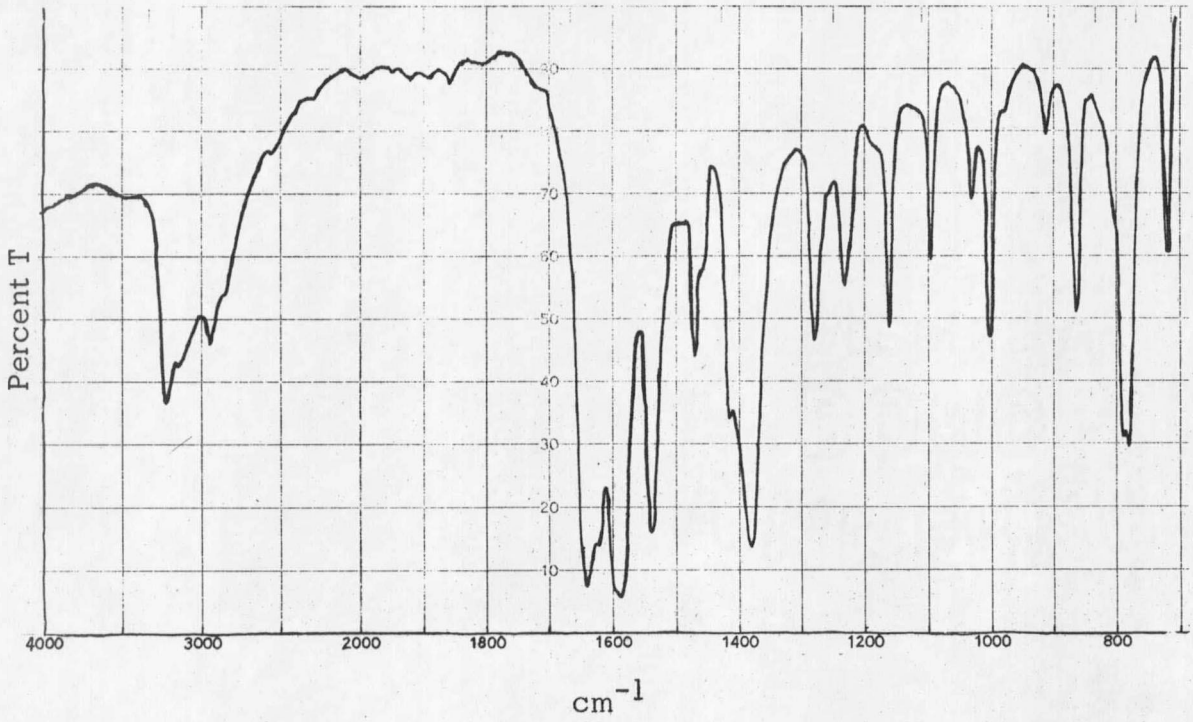

Figure 36. Infrared Spectrum of $CuCl_2 \cdot 2\,C_5H_5NO$

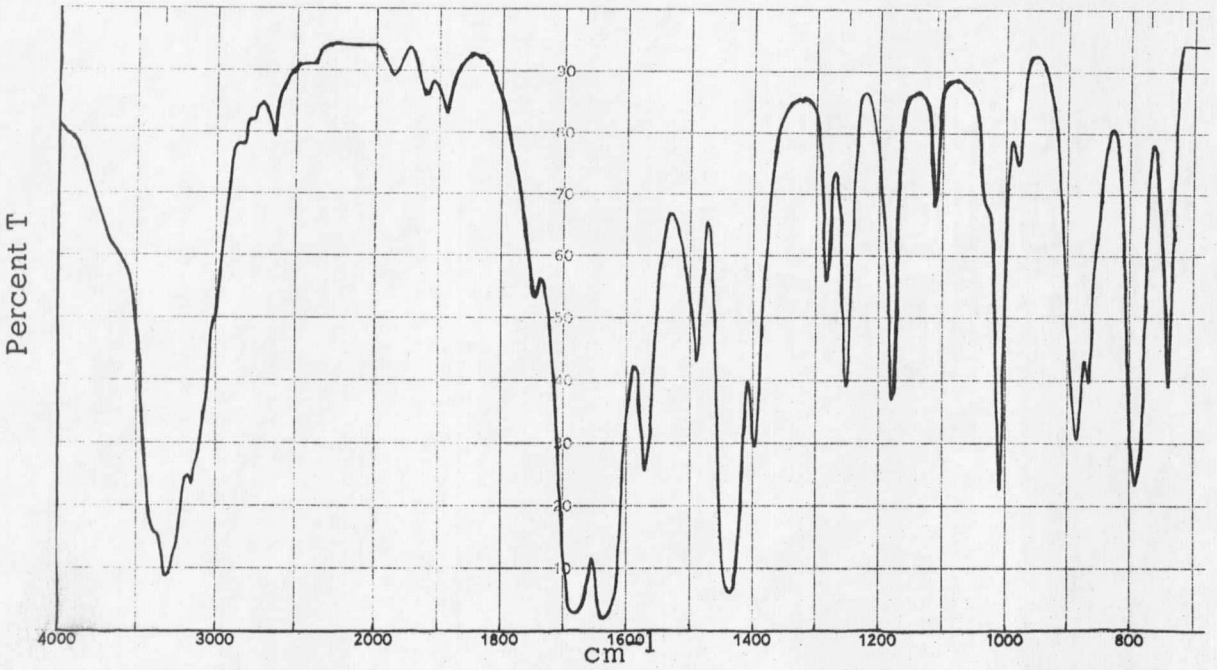

Figure 37. Infrared Spectrum of $CoCl_2 \cdot 3C_5H_5NO$

The magnetic susceptibilities and moments for the complexes appear in Table XIV.

Table XIV

$CuCl_2 \cdot 2C_5H_5NO$ and $CoCl_2 \cdot 3C_5H_5NO$

Magnetic Susceptibilities and Moments

Complex	Temp.	X_m(cgs, esu) $\times 10^6$ Magnetic Susceptibility	(B.M.) Magnetic Moment
$CuCl_2 \cdot 2C_5H_5NO$	80°	4,700	1.76
	210°	2,500	2.06
	250°	2,100	2.06
	298°	1,400	1.82
$CoCl_2 \cdot 3C_5H_5NO$	80°	32,200	4.59
	210°	13,800	4.87
	250°	11,400	4.82
	298°	9,600	4.85

DISCUSSION

Dichloro-mono-α-pyridone Metal(II) Complexes

The infrared spectra of the $MCl_2 \cdot 1\,C_5H_5NO$ complexes (Figures 25-28, pages 30-32) show shifts in absorption energies and intensities in important regions of the spectrum. Katritsky (30), Mason (31) and others (32-38) have examined the infrared spectra of α-pyridone and have assigned most of the observed absorption bands to the vibrations expected to occur within the molecule. The accepted literature values for α-pyridone are shown in Table XV with the bands observed in this study for α-pyridone and the four $MCl_2 \cdot 1\,C_5H_5NO$ compounds (Figures 25-28, pages 30-32). The symbols υ, β and γ are those used by Mason; υ represents the fundamental stretching vibration between bonded atoms. β represents the in-plane-bending vibration and γ represents the out-of-plane bending vibration. The shifts observed in the absorption energies and intensities in the υN-H, υC = 0, βN-H and γN-H regions indicate that α-pyridone is probably coordinated to the metal ions through the oxygen atom. Free α-pyridone has been shown to be a hydrogen bonded dimer (Figure 38) in the crystalline state (30). The υN-H peak in crystalline α-pyridone is broad and at lower energies (due to intermolecular hydrogen bonding) than normally expected for free υN-H vibration; a free υN-H peak normally appears at 3400 cm^{-1}. If the υN-H peak shifts to higher energies, this is an indication of increased free N-H and decreased hydrogen bonding; it suggests that coordination is not occurring at the nitrogen atom. All four α-pyridone complexes exhibit υ-NH shifts to higher energies (3100 $cm^{-1} \longrightarrow$

Table XV

Infrared Band Assignments $MCl_2 \cdot 1C_5H_5NO$ Complexes

Assignment	Lit. Values	α-pyridone	Cu(II)	Co(II)	Ni(II)	Mn(II)
νN-H	3200-3100 strong, broad	3100s*	3250m 3150m	3225b 3150s	3250s 3150w	3450s
νC=O	1665-1650s	1685s	1655m	1645m	1600s	1685s
νRing.Freq.	1619-1570s	1615m	1610s	1602s	1610s	1640s
	1560-1585m		1550w	1545m	1550m	1570m
	1501-1472w(m)	1460w	1475w	1465w	1465m	1485w
	1455-1415w(m)	1440m	1415s	1405s	1420s	1440s
β-N-H (amido N-H)	1600m	1615m	1610s	1602s	1610s	1640s
β-C-H	1318-1242m	1245s	1278m	1285m	1280m	1290m
	1182-1154m	1160s	1170w	1170m	1170s	1185s
	1144-1138m	1100s	1105w	1105w	1100m	1110m
	1018-1010w	1010w	1010w	10102	1005s	1010s
γCH	842-832m	850w	865m	865m	865s	870s
γNH	820 region	785s	775s	780s	775s	780s
	720 region	735s	730s	720m	725s	730s

*s=strong, m=medium, w=weak, b=broad

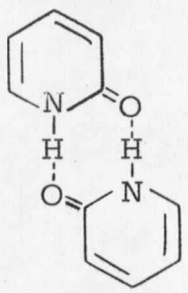

Figure 38. α-pyridone (C_5H_5NO) Structure

3150-3250 cm^{-1}). The βN-H and γN-H peak shifts also support decreased hydrogen bonding and increased free N-H; that is, less energy would be required for these deformations in a non-hydrogen bonded compound. The shift in all of these peaks was small and the νN-H peak was still far enough from 3400 cm^{-1} to suggest some hydrogen bonding might still be involved. The position of the νC = O peak in crystalline α-pyridone is again indicative of hydrogen bonding; free νC=O peak normally appears at higher energies, >1700 cm^{-1}. Therefore, a νC=O peak shift indicates a change in bonding has occurred at the oxygen atom. The frequency of a νC=O vibration in compounds where the oxygen is coordinated to another atom or group of atoms is dependent upon the mass of the coordinating group, i.e. an increased mass will lower the frequency. Therefore, if α-pyridone is coordinated to a metal ion through the carbonyl oxygen, the νC=O peak would be expected to shift to lower frequencies. Such a shift was generally observed for the $MCl_2 \cdot 1C_5H_5NO$ compounds. Absorption peaks around 1600 cm^{-1} have been assigned to ν ring vibrations and βN-H vibrations (30). Fundamental ring vibrations should not be affected by coordination to metal ion, but the βN-H vibration (in-plane band) of α-pyridone would be affected. The intensity of this peak is increased and shifted to slightly lower frequencies, which suggests that the βN-H vibration has become less hindered. These changes in the infrared absorption bands seemed to indicate that α-pyridone was coordinating to the metal ions through the oxygen atom.

The ultraviolet absorption bands of the mono-α-pyridone complexes (Table VII, page 21) are in good agreement with those reported by Mason (40)

for α-pyridone; λmax. 224, 293 mμ. There was a general decrease, however, in the molar absorptivities of these bands in the complexes. The 224 mμ band (ϵ_{max} = 7230) and 293 mμ bands (ϵ_{max} = 5890) have been assigned by Mason as characteristic $\pi \rightarrow \pi^*$ and $\eta \rightarrow \pi^*$ carbonyl electronic transitions. Coordination to a metal ion generally decreases the molar absorptivities of these transitions. Therefore, the ultraviolet spectra of the $MCl_2 \cdot 1C_5H_5NO$ complexes seemed to indicate the oxygen atom was coordinated to the metal ion.

Molecular weight determinations of the Cu, Co and Ni complexes are rather inconclusive. The ebullioscopic results indicate the complexes dissociate at elevated temperatures; osmometric results suggest the complexes might be tetrameric or even higher polymeric species.

X-ray powder diffraction patterns clearly indicated that the four complexes have similar structures. The data listed in Table VI, page 20, show that the Co, Ni and Mn complexes are isomorphic. The data also indicated some differences between the Cu complex and the other three complexes. However, it is clear that the structure of the Cu complex is similar to the others. Single crystal x-ray diffraction data indicated that there is a close relationship between the Cu and Co compounds. The structure of the Cu compoud has been determined from a two-dimensional projection of single crystal data gathered and treated by normal crystallographic procedures. The unit cell dimensions of the Cu compound are a = 9.93 Å, b = 9.94 Å, c = 3.95 Å and γ = 113.2°; the structure will be discussed in greater detail later in the thesis. The unit cell dimensions of the Co compound, a = 24.8 Å,

b = 16.7 Å, c = 8.7 Å, have also been determined from single crystal data and a three-dimensional analysis is now under way. The dimensions for the Cu and Co compounds appear quite different; however, they may be related, as shown in Figure 39, by the following:

$$A = 2\sqrt{a^2 + b^2 - 2ab\cos(180^\circ - \gamma)}$$

$$B = \sqrt{a^2 + b^2 - 2ab\cos\gamma}$$

$$C = 2c$$

The capital letters represent the Co compound; small letters represent the Cu compound.

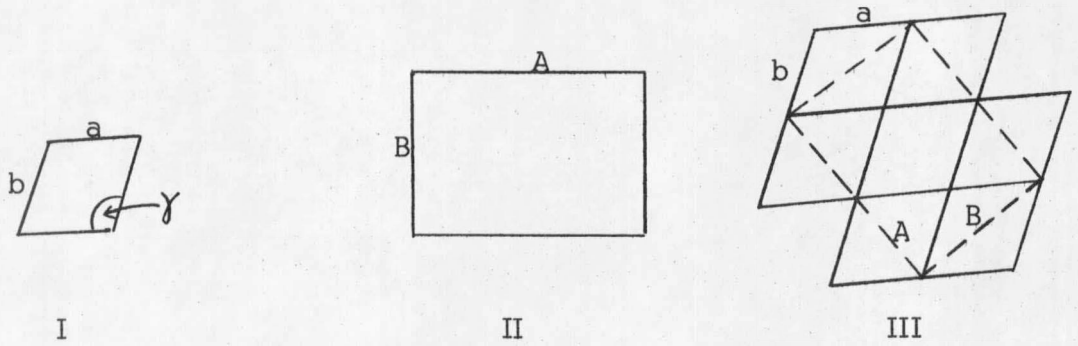

Figure 39. Unit Cell Relationship of Cu and Co Compounds

I shows the general shape of the $CuCl_2 \cdot 1C_5H_5NO$ unit cell; II, the $CoCl_2 \cdot 1C_5H_5NO$ unit cell; III, the relationship between I and II; the third axes, c and C, are perpendicular to the plane of the paper. Solution of the equations by using the appropriate Cu values, gives A = 22 Å, B = 16.6 Å, C = 8 Å. These values are reasonably close to the observed values for the Co compound. The observed value (8.7 Å) for the c axis in the Co compound

is approximately ten per cent longer than the calculated value. The increased length may be due to a different molecular packing in the crystal; that is, the molecules in the Cu compound are all oriented in the same manner and nest one on top of the other. If the molecules do not nest, out-of-plane distortions would require greater molecular separation and therefore a larger crystal axis. The increased length of the a axis compared to the calculated value is also thought to be a function of the molecular packing, but is as yet not completely understood. These relationships strongly suggest that the molecular unit in the two structures is the same.

Dichloro-mono-α-pyridone Copper(II)

Single crystal x-ray diffraction data indicates the structure of $CuCl_2 \cdot 1C_5H_5NO$ is as shown in Figure 40.

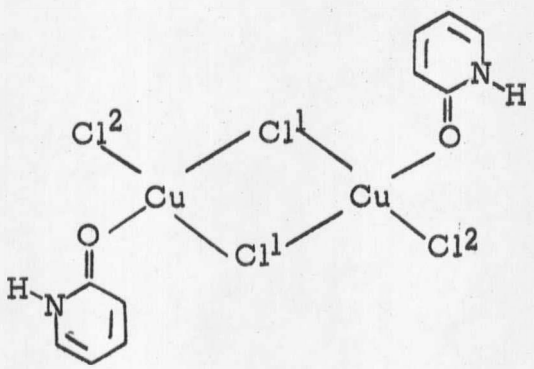

Figure 40. $CuCl_2 \cdot 1C_5H_5NO$ Structure

The compound is definitely dimeric. The bridging chlorine atoms and the Cu atoms are all in the same plane; the Cu-Cu distance is approximately 3.23 Å,

Cu-Cl^1 distances are approximately 2.2 Å. The Cu-Cl^2 distance is approximately 1.6 Å in projection. This distance is much too short and may indicate that this chlorine atom is not in the same plane. The Cu-O distance, in projection, is also too short and suggests that the oxygen atom is not in the same plane. Additional refinement of the available data is required before the positions of Cl^2 and O atoms and the α-pyridone rings can be determined. The refinement process is now in progress. With the information at hand, it appears the environment of the Cu atoms is probably square planar or distorted tetrahedral. The structure of the complex as presented supports the conclusion drawn from interpretation of the infrared and ultraviolet spectra that α-pyridone was bonded through the oxygen atom.

The magnetic moment of the Cu Complex (1.93 B.M.) has been determined at 80° and 298°K and appears to be temperature independent. A few compounds containing chlorine-bridged copper atoms have been previously identified and investigated. $CsCuCl_3$ (1.93 B.M.) has been assigned a distorted octahedral structure by Figgis and Harris (41) and Schluetter and co-workers (42). Figgis and Harris have suggested that magnetic moments of tetrahedral Cu complexes might be higher than the magnetic moments for square planar Cu complexes. Cs_2CuCl_4 (2.00 B.M.) is a distorted tetrahedron (41), $[Pt(NH_3)_4]\,[CuCl_4]$, known to have a square planar structure (43, 44), has a magnetic moment of 1.77 B.M. $CuCl_2$ (1.75 B.M.), Figure 43, has an infinite, planar, chlorine-bridged chain structure (45). Successive chains are offset so that chlorine atoms in adjacent chains fall above and below each copper atom giving a distorted octahedral arrangement. It has been

suggested (46) that the lower magnetic moment for $CuCl_2$ is due to a super exchange pathway via bridging chlorine atoms between chains. A distorted tetrahedral structure for $CuCl_2 \cdot 1 C_5H_5NO$ appears to be more probable instead of a square planar structure when the suggestion of Figgis and Harris and the magnetic moments of known tetrahedral and square planar chlorine bridged Cu(II) compounds are considered. The x-ray crystal data indicates that the dimers are stacked one on top of the other, giving chains of Cu atoms thus eliminating the possibility of chlorine-bridges between layers of dimers to form an octahedral Cu environment similar to $CuCl_2$. Therefore, a lower moment is not expected for $CuCl_2 \cdot 1 C_5H_5NO$. Since there are known octahedral and tetrahedral chlorine-bridged Cu(II) compounds with similar magnetic moments, it is not possible at this time to assign either a distorted octahedral or tetrahedral structure to $CuCl_2 \cdot 1 C_5H_5NO$.

The visible spectra (Figures 12-14, pages 22, 23) of $CuCl_2 \cdot 1 C_5H_5NO$ exhibit maxima at 450 mμ (CH_3CN), 790 mμ (H_2O) and 880 mμ (C_3H_5OH). Several Cu(II) compounds exhibit maxima in these regions as shown in Table XVI; the first seven compounds contain chlorine-bridged Cu atoms. On the basis of the visible spectra, a distorted tetrahedral structure might be favored for $CuCl_2 \cdot 1 C_5H_5NO$.

Diffuse reflectance spectra have been used to obtain approximate absorption spectra of solids in the visible or near ultraviolet regions. The reflectance and absorption spectra are not always identical, but progress has been made in the interpretation of reflectance spectra. The diffuse reflectance spectrum of $CuCl_2 \cdot 1 C_5H_5NO$ (Figure 21, page 28) shows a maximum

Table XVI

Visible Absorption Bands of Some Representative Cu(II) Compounds

Compound or Species	λ max mμ	Assigned Configuration	Reference
Li_2CuCl_4	450	Dist. tetrahedral	(47)
Li_2CuCl_4	375	Planar	(47)
$[CH_3C(NH_2)_2]CuCl_4$	450	Tetrahedral	(48)
Cs_2CuCl_4	405	Dist. tetrahedral	(49)
$(2\text{-}CH_3\text{-}C_5H_4N)_2CuCl_2$[a]	746 804	Dist. tetrahedral	(50)
$CsCuCl_3$	408	Dist. octahedral	(51)
$[Pt(NH_3)_4][CuCl_4]$	402 700 765	Square planar	(44)
$Cu(C_6H_5N{:}NN{:}C_6H_5)_2$[b]	667 525	Square planar	(52)
$CuCl_2 \cdot 1\,C_5H_5NO$[c]	789-790 430-455	Dist. tetrahedral	(12)
$CuCl_2 \cdot 1\,R\text{-}C_5H_4NO$[c]	750-800 430-470	Dist. tetrahedral	(12)

[a] 2-methylpyridine
[b] diazoaminobenzene
[c] pyridine-N-oxide

in the 425-450 mμ region. Ros (51) has found a maximum at 408 mμ in the diffuse reflectance spectrum of $CsCuCl_3$ (distorted octahedral). $CuCl_2 \cdot 1\,C_5H_5NO$ (pyridine-N-oxide), Figure 1, page 3, has a distorted tetrahedral structure. Muto and Jonassen (12), as previously mentioned, have prepared Cu(II) compounds with substituted pyridine-N-oxide ligands.

They have found that the diffuse reflectance spectra of the compounds assumed to have a distorted tetrahedral structure exhibit maxima in the 400-435 mμ region. Therefore, in view of the data presented by Ros and Johassen, a distorted tetrahedral structure for $CuCl_2 \cdot 1\,C_5H_5NO$ appears more likely than a distorted octahedral structure.

The x-ray single crystal data clearly indicate that there is no linkage between Cu atoms in adjacent dimers as in $CuCl_2$ chains and that only the non-bridging chlorine atoms appear to fall out of the plane. Although only a complete three-dimensional x-ray analysis will unequivocally establish the structure of $CuCl_2 \cdot 1\,C_5H_5NO$, it appears that available x-ray, visible solution and diffuse reflectance spectral data support a distorted tetrahedral structure for this complex.

Dichloro-mono-α-pyridone Cobalt(II)

The single crystal x-ray diffraction data for the Co complex have not reached the stage of refinement of the Cu compound, but some characteristics of the structure of the Co compound are known. Since the unit cells of these two compounds are related as shown in Figure 39, page 45, the Co compound is probably also a chlorine bridged dimer and is expected to have a distorted tetrahedral structure similar to that proposed for the Cu compound.

The magnetic moment of the Co compound is 5.39 B.M. at 298°K. The calculated spin only magnetic moment for spin free Co(II) is 3.88 B.M. The room temperature magnetic moments for several known Co(II) compounds are shown in Table XVII. It is immediately obvious that the magnetic moments

Table XVII

Room Temperature Magnetic Moments for Co(II) Compounds

Compound or Species	Assigned Config.	Magnetic Moment(B.M.)	Reference
$(NH_4)_2Co(SO_4)_2 \cdot 6H_2O$	Octahedral	5.1	(53)
$CoCl_4^=$	Octahedral	4.8-5.2	(54)
$Co(CH_3CN)_6^{++}$	Octahedral	4.9-5.6	(55)
$CoCl_2 \cdot 2(CH_3C_5H_4N)$	Tetrahedral	4.8	(56)
Cs_2CoCl_4	Tetrahedral	4.5	(53)
$CoCl_4^=$	Tetrahedral	4.69	(54)
$CoCl_4^=$	Tetrahedral	4.6-4.9	(57)
CoX_4^{-2}	Tetrahedral	4.3-4.8	(55)
$CoCl_2 \cdot 2(2,6DMPNO)^a$	Tetrahedral	4.59	(58)
$CoCl_2 \cdot 1$ dipyridylamine	Tetrahedral	4.51	(59)
Co(phthalocyanine)	Square Planar	2.4	(53)

of these compounds are quite different from the calculated spin-only value. Spin only values are calculated from the expression (53):

$$B.M. = \sqrt{4S(S+1)}$$

$$S = \text{total spin quantum number}$$

This expression is derived from the theory for a free metal ion (no external perturbing fields) by omitting orbital angular momentum and considering only spin angular momentum of the electron. Electrons occupying an orbital exhibit both spin angular momentum and orbital angular momentum. An unpaired electron always contributes its spin angular momentum to the

magnetic moment of an ion; an electron may contribute its orbital angular momentum to the magnetic moment if there is a rotationally equivalent orbital that can accept the electron. That is, the Pauli exclusion principle must be obeyed; no two electrons with the same spin can occupy the same orbital. This means, therefore, that the rotationally equivalent orbital may be unoccupied or if occupied, the electron being transferred must be of opposite spin to the electron in the orbital. It has also been shown that spin-orbit coupling contributes to the magnetic moment of an ion (53,57,58). Russell-Saunders spin-orbit coupling increases the degeneracy (number of rotationally equivalent orbitals) of the electronic states of an ion and this also contributes to the magnetic moment of the ion. The Co(II) compounds listed in Table XVII have magnetic moments greater than the calculated spin only value. This indicates that some electrons are contributing their orbital angular moments to the magnetic moment. Orbital angular momentum contributions alone cannot account for the large differences observed, and spin-orbit coupling must also be contributing to the magnetic moment of these complexes. It is obvious from the data in Table XVII that octahedral complexes exhibit greater orbital and/or spin-orbit coupling contributions to the magnetic moment than either tetrahedral or square planar complexes. The magnetic moment of $CoCl_2 \cdot 1C_5H_5NO$ is higher than observed values for several octahedral Co(II) complexes. The reason for the high moment remains unexplained. The magnetic data appears to support an octahedral structure for $CoCl_2 \cdot 1C_5H_5NO$ rather than a tetrahedral structure.

Libus and Uruska (60) state that tetrahedral Co(II) compounds exhibit characteristic absorption bands at 576, 608 and 638 mμ. The molar absorptivities of tetrahedral Co(II) absorption bands are generally larger than 100. The molar absorptivities of octahedral Co(II) absorption bands are generally smaller than 100. In addition, octahedral (Co(II) species generally exhibit a low intensity band around 515 mμ that does not appear with tetrahedral Co(II) compounds (60). The configuration of Co(II) ions in solution is dependent upon the coordinating strength (ligand field strength) of the solvent; weakly coordinating solvents yield tetrahedral species, strongly coordinating solvents produce octahedral species (Table XVIII). The absorption bands for several known Co(II) compounds are listed in Table XVIII.

Table XVIII

Visible Solution Spectra of Known Co(II) Compounds

Compound or Species	Solvent	λ max mμ	Config.	References
$CoCl_4^{-2}$	CH_3NO_2	593, 613(sh), 635		(54)
$CoCl_4^{-2}$	------	668, 693	Tetrahedral	(57)
CoX_4^{-2}	CH_3CN	680	Tetrahedral	(55)
$CoCl_2$	$(CH_3)_2CO$	575, 630(sh), 674	Tetrahedral	(61)
$CoCl_2 \cdot 2\,C_5H_5N$	$CHCl_3$	579, 611, 638-662	Tetrahedral	(56)
$CoCl_2$	C_5H_5N	576, 608, 638	Tetrahedral	(60)
$Co(CH_3CN)_6^{++}$	CH_3CN	570, 610	Octahedral	(55)
$CoCl_2$	H_2O	465, 513	Octahedral	(62)
$CoBr_2 \cdot 2\,R\text{-}C_5H_4NO$	CH_3OH	530, 600(sh), 620	Octahedral	(58)
$Co(ClO_4)_2$	H_2O	513	Octahedral	(63)
	$(CH_3)_2CO$	512	Octahedral	(63)
	C_2H_5OH	515	Octahedral	(63)

$CoCl_2 \cdot 1C_5H_5NO$ has an absorption maximum at 638 mμ with shoulders at 575, 612, 655 and 665 mμ in C_2H_5OH; maxima at 556, 590 and 660 mμ with shoulders at 570, 610 and 650 in CH_3CN. The molar absorptivities for these bands shown in Table VIII, page 27, are larger than 100. The absorption bands for $CoCl_2 \cdot 1C_5H_5NO$ agree reasonably well with those reported in Table XVIII for tetrahedral Co(II) compounds in solvents with low dielectric constants. The low intensity band around 515 mμ observed for octahedral Co(II) compounds is missing in $CoCl_2 \cdot 1C_5H_5NO$ electronic spectra. Therefore, on the basis of the data presented, it appears that solutions of $CoCl_2 \cdot 1C_5H_5NO$ in CH_3CN and C_2H_5OH contain tetrahedral Co(II) species.

The diffuse reflectance spectrum of $CoCl_2 \cdot 1C_5H_5NO$, Figure 22, page 28, is similar to its solution spectra. The complex has reflectance maxima at 450, 545, 585 and 620 mμ with a shoulder at 520 mμ. The diffuse reflectance bands for known Co(II) compounds are shown in Table XIX. King (56) has noted similarities between reflectance and solution spectra of pyridine compounds of Co(II). Jonassen, in contrast to King, has noted marked differences between reflectance and solution spectra, but he suggests that this can be used as an indication that the compound has a different configuration in the solid state than when in solution (12). However, King dissolved his compounds in $CHCl_3$ and Jonassen dissolved his in CH_3OH and other solvents with high dielectric constants and coordinating strength. This suggests that the structure of a compound in the solid state might very well retain that structure in a weakly coordinating solvent. The complexes

Table XIX

Diffuse Reflectance Bands of Known Co(II) Compounds

Compound or Species	λmax mμ	Assigned Config.	References
$CoCl_2 \cdot 2H_2O$	510, 620	Octahedral	(64)
$CoCl_2 \cdot 2(CH_3\text{-}C_5H_4N)$	585(sh), 615(sh), 637	Tetrahedral	(56)
$CoCl_2 \cdot 2C_5H_5N$	513(sh), 526, 541, 620	Bridged Octahedral	(65)
$CoCl_4^=$(in fused salts)	600, 637, 676	Octahedral	(66)
$CoCl_4^=$(in fused salts)	595, 650, 735	Distorted Octahedral	(66)
$CoCl_4^=$(in fused salts)	630, 670, 700	Distorted Octahedral	(66)
$CoCl_2 \cdot 1$ dipyridylamine	541, 559, 606	Tetrahedral	(59)
$CoCl_4^=$(single crystal spectra)	715-589 region	Distorted Tetrahedral	(65)
	582-500 region		
	455-415 region		

$CoCl_2 \cdot 1$ dipyridylamine and $CoCl_2 \cdot 2(CH_3\text{-}C_5H_4N)$ contain ligands that are similar to α-pyridone and their reflectance spectra agree reasonably well with the $CoCl_2 \cdot 1C_5H_5NO$ spectrum. Also, Ferguson indicates that known distorted tetrahedral $CoCl_4^=$ species exhibit absorption bands in three distinct regions of the spectrum (Table XIX). Octahedral Co(II) species generally have reflectance bands above 600 mμ while tetrahedral Co(II) species generally have reflectance bands below 600 mμ. There is open disagreement in the literature concerning interpretation of reflectance spectra, but in view of the results reported by King, Ferguson (67) and M. Goodgame, it

appears the reflectance data support the conclusion that $CoCl_2 \cdot 1\,C_5H_5NO$ is a tetrahedral compound.

Except for the magnetic moment, the data assembled appear to support the tetrahedral structure proposed for $CoCl_2 \cdot 1\,C_5H_5NO$ from x-ray diffraction data. The magnetic moment is higher than any other reported moment for a tetrahedral Co(II) compound and appears to favor an octahedral structure. However, the understanding of orbital angular momentum and spin-orbit coupling contributions to the magnetic moment of Co(II) complexes is still very incomplete and the magnetic moment, alone, should not be used as a criterion in assignment of configurations. The composite data indicate that $CoCl_2 \cdot 1\,C_5H_5NO$ is probably a tetrahedral compound.

Dichloro-mono-α-pyridone Nickel(II)

The x-ray powder diffraction data listed in Table VI, page 20, indicate that $CoCl_2 \cdot 1\,C_5H_5NO$ and $NiCl_2 \cdot 1\,C_5H_5NO$ are isomorphic. Therefore, since $CoCl_2 \cdot 1\,C_5H_5NO$ is isostructural to $CuCl_2 \cdot 1\,C_5H_5NO$, the Ni compound is also expected to be a chlorine bridged dimer with a distorted tetrahedral Ni(II) environment.

The magnetic moment of the Ni complex (3.65 B.M.) is temperature dependent. The moment exhibits a steady increase as the temperature is lowered (Table V, page 20). This type of behavior is characteristic of tetrahedral Ni(II) compounds (68). The magnetic moments of several Ni(II) compounds are known and some of them are listed in Table XX. King and coworkers (56) and Lever (68) state that tetrahedral Ni(II) complexes have

Table XX

Magnetic Moments of Some Ni(II) Compounds

Compound or Species	Magnetic Moment(B.M.)	Assigned Configuration	References
$(NH_4)_2Ni(SO_4)_2 \cdot 6H_2O$	3.3	Octahedral	(53)
$Ni(H_2O)_6^{++}$	2.9-3.2	Octahedral	(54)
$Ni(NO_3)_2 \cdot 3C_5H_5N$	3.21	Octahedral	(69)
$NiCl_2 \cdot C_5H_5N$	3.47	Bridged Octahedral	(70)
$NiCl_2 \cdot 2C_5H_5N$	3.37	Bridged Octahedral	(56)
$NiCl_2 \cdot 2C_5H_5N$	3.39	Bridged Octahedral	(70)
$Ni[tremme]^{a}_3Cl_2$	3.42	Trigonal Bipyramid	(71)
$(Et_4N)_2NiCl_4$	3.8	Tetrahedral	(53)
$NiCl_4^{=}$	3.87	Tetrahedral	(54)
$Ni[(CH_3)_3NO]_4(Cl_4)_2$	3.86	Tetrahedral	(72)
$NiCl_2 \cdot 2$ Quinoline	3.54	Tetrahedral	(73)
$(BuPh_2P)^{b}_2NiCl_2$	3.35	Tetrahedral	(74)
$K_2Ni(CN)_4$	0	Square Planar	(53)

[a] 2-dimethyl-aminoethylamine
[b] butyl-dipheylphosphine

magnetic moments of 3.3-4.2 B.M. Square planar Ni(II) compounds are generally diamagnetic; therefore, it appears safe to eliminate a square planar configuration for the α-pyridone complex in view of the data presented. The data also indicate that some octahedral Ni(II) compounds have magnetic moments that fall within the range quoted for tetrahedral Ni(II) compounds.

However, none of these compounds have moments that are temperature dependent. Therefore, the magnetic moment of $NiCl_2 \cdot 1\,C_5H_5NO$ supports the proposed tetrahedral structure.

The solution spectra of the Ni complex show absorption maxima at 385 and 700 (very broad) mμ in H_2O; 413 and 760 (very broad) mμ in C_2H_5OH; 412, 600 and 675 mμ in $HCON(CH_3)_2$. The literature contains many studies of Ni(II) compounds which have used electronic spectra to help determine molecular configuration (54, 60, 63, 69-72, 74-77). The absorption bands for tetrahedral and octahedral Ni(II) species overlap to a large extent and make assignment of a configuration difficult. However, the molar absorptivities of octahedral Ni(II) complexes are generally less than 100, while molar absabsorptivities of tetrahedral Ni(II) complexes are generally more than 100. The molar absorptivities for $NiCl_2 \cdot 1\,C_5H_5NO$ shown in Table VIII, page 27, are low, but the maxima agree with those observed for both configurations. The observed configuration for Ni(II) species in solution also appear to be dependent upon the coordinating strength of the ligand and solvent used as is the case with Co(II). $NiCl_2 \cdot 1\,C_5H_5NO$ is insoluble in weakly coordinating solvents (C_6H_6, $CHCl_3$, CH_3NO_2, dioxane) which makes it difficult to check the possibility that $NiCl_2 \cdot 1\,C_5H_5NO$ might yield a specific Ni(II) species in this type of solvent. However, in light of the observed absorptivities for $NiCl_2 \cdot 1\,C_5H_5NO$ absorption bands, there is probably an octahedral Ni(II) species in solution.

The α-pyridone compound has a broad reflectance maximum between 450-470 mμ. Known octahedral and tetrahedral Ni(II) compounds both have

reflectance maxima in this region plus additional maxima on either side of that band. Studies by Allen and co-workers (78) and Nelson and Shepard (70) with $NiCl_2 \cdot X C_5H_5N$ yield the best agreement with the α-pyridone band, but their reflectance spectra exhibit several bands between 350-700 mμ (the limits of this study). Their compounds have been assigned distorted octahedral structures. It should be noted that there is a difference between the reflectance band and the solution bands for the α-pyridone compounds. However, as previously mentioned, this suggests a change in configuration when the solid is dissolved and the change appears to be dependent upon the solvent used. At best, the reflectance spectrum of $NiCl_2 \cdot 1 C_5H_5NO$ supports an octahedral structure but is by no means conclusive.

The solution and reflectance spectra of $NiCl_2 \cdot 1 C_5H_5NO$ when compared with spectra of known Ni(II) compounds offer little assistance in the assignment of a specific configuration for the complex in the solid state. Additional investigation is necessary before these spectra will benefit the study. On the other hand, the x-ray diffraction data and especially the magnetic moment data both very clearly support a tetrahedral structure for $NiCl_2 \cdot 1 C_5H_5NO$ in the solid state.

Dichloro-mono-α-pyridone Manganese(II)

Tetrahedral structures have been proposed for the Cu, Co and Ni members of the $MCl_2 \cdot 1 C_5H_5NO$ series prepared in this study. The remaining member of the series, $MnCl_2 \cdot 1 C_5H_5NO$, probably also has a tetrahedral structure because x-ray powder diffraction data show it to be

isomorphic to the Co and Ni compounds. It, too, is expected to be a chlorine-bridged dimer.

The magnetic moment of the Mn complex (5.97 B.M.) is very close to the calculated spin-only moment of 5.9 B.M. for a spin free Mn(II) ion (53). The moment of the complex is temperature independent and appears to follow the Curie-Weiss Law. Both octahedral $K_2Mn(SO_4)_2 \cdot 6H_2O$ and tetrahedral $[(C_2H_5)_4N]_2MnCl_4$ have magnetic moments of 5.9 B.M. (53). There was recently reported (79) a five-coordinate Mn(II) compound with a trigonal bipyramid structure and a magnetic moment of 5.85 B.M. It appears, therefore, since these known values are so close, that magnetic data for Mn(II) compounds will not permit differentiation between specific structural configurations. The magnetic moment of $MnCl_2 \cdot 1C_5H_5NO$ indicates only that the complex contains spin free Mn(II) ions.

The diffuse reflectance spectrum of $MnCl_2 \cdot 1C_5H_5NO$ has band maxima at 365, 455, and a very broad band, 505-560 mμ that appears to be centered around 530 mμ. Cotton and co-workers (80) have reported diffuse reflectance spectra for three Mn(II) compounds that have been assigned tetrahedral structures. They show that the reflectance maxima appear in three distinct regions: 360-385 mμ, 430-455 mμ, and 470-480 mμ. The trigonal bipyramid Mn(II) compound mentioned above has reflectance maxima at 371 and 435 mμ. No solution spectra were obtained for $MnCl_2 \cdot 1C_5H_5NO$ in this study, but it should be noted that tetrahedral $MnCl_4^=$ solution spectra reported by Furlani and Furlani (81) are almost identical to the reflectance spectra reported by Cotton and co-workers. Allen and co-workers (83) have

reported solution absorption maxima at 540, 460 and 430 mμ for chlorine-bridged octahedral Mn(II) compounds. The $MnCl_2 \cdot 1C_5H_5NO$ reflectance data agrees reasonably well, within the limits of the study, with that reported for known tetrahedral Mn(II) compounds and seem to support a tetrahedral configuration rather than an octahedral configuration.

Solution spectra were not obtained for the Mn(II) complex because it is much less soluble in the common spectral solvents than the Cu, Co and Ni complexes. The intensities of the Mn(II) bands, d-d transitions, generally observed in the visible and near infrared regions of the spectrum are weak and the bands are very sharp. These transitions are forbidden transitions for d electrons. That is, they are forbidden by the multiplicity (spin) and Laporte selection rules for electronic transitions. Many transition metal ions are identified by absorption bands in the visible region of the spectrum which have been attributed to d-d transitions. The Laporte selection rule specifically forbids such transitions for a free metal ion, but a coordinated metal ion undergoes mixing of d and p orbitals to a sufficient degree that now an allowed d → p transition may occur, but will be less intense than completely allowed transitions. A spin forbidden transition requires an electron to change its spin when it enters an orbital that is already occupied by a single electron. Such a change decreases the multiplicity of the state and is therefore forbidden. A Mn(II) ion, spin free, is already at its maximum multiplicity. The bands observed in Mn(II) solution spectra and diffuse reflectance spectra are probably spin forbidden d-d, allowed d-p, and/or charge transfer (ligand → metal) transitions. The d-d

transitions generally occur at lower energies than d-p or charge transfer transitions. The d-d transitions observed for tetrahedral Mn(II) compounds would be more intense than for octahedral compounds because a center of symmetry, as in an octahedral complex, destroys d-p orbital mixing. If a transition is weak, a more concentrated solution is required for electronic spectral analysis. The quantity of the Mn complex was limited so extensive electronic investigation was hindered. Again, only a single crystal x-ray analysis will exactly show the structure of $MnCl_2 \cdot 1\,C_5H_5NO$, but the data gathered to date indicate it is probably a tetrahedral compound.

Dichloro-n-α-pyridone Metal(II) Complexes

The ultraviolet solution spectra of the complexes, $CuCl_2 \cdot 2\,C_5H_5NO$ and $CoCl_2 \cdot 3\,C_5H_5NO$, differ from that of free α-pyridone much as do those for the complexes previously described for the $MCl_2 \cdot 1\,C_5H_5NO$ compounds. The infrared spectra of these compounds shown in Figures 36 and 37, pages 39 and 40, also show band and intensity shifts similar to the complexes just discussed; Table XXI lists the infrared bands for these complexes. Therefore, the α-pyridone is probably bonded through the oxygen atom to the metal ion in these complexes as well.

The x-ray powder diffraction data for these complexes shown in Table XI, page 34, indicate differences in intensities and θ angles when compared with the powder diffraction data for $CuCl_2 \cdot 1\,C_5H_5NO$ and $CoCl_2 \cdot 1\,C_5H_5NO$. The powder data suggest that $CuCl_2 \cdot 2\,C_5H_5NO$ and $CoCl_2 \cdot 3\,C_5H_5NO$ have different structures than $CuCl_2 \cdot 1\,C_5H_5NO$ and $CoCl_2 \cdot 1\,C_5H_5NO$.

Table XXI

$CuCl_2 \cdot 2\,\alpha$-pyridone and $CoCl_2 \cdot 3\,\alpha$-pyridone Infrared Bands

M	νN-H	νC=O	Ring Freq.	(amido N-H) βN-H	βC-H	γC-H	γN-H
Cu(II)	3225(m)	1640(s)	1590(s)	1590(s)	1280(m)	865(s)	780(s)
			1540(s)		1160(s)		720(s)
			1470(m)		1095(m)		
			1380(s)		1005(m)		
Co(II)	3300(s)	1680(s)	1635(s)	1635(s)	1280(m)	885(s)	790(s)
			1570(m)		1180(s)		740(s)
			1490(m)		1110(m)		
			1440(s)		1010(s)		

s = strong, m = medium

As previously mentioned, no effort was made to determine the molecular weight of these complexes.

Dichloro-bis-α-pyridone-Copper(II)

The diffuse reflectance spectrum of $CuCl_2 \cdot 2\,C_5H_5NO$ shown in Figure 34, page 38, does not show any definite maxima. A shoulder appears around 700 mμ, but data could not be obtained beyond this point. Therefore, it appears the reflectance spectrum does not provide useful data for assignment of a specific configuration to $CuCl_2 \cdot 2\,C_5H_5NO$.

The visible solution spectra of $CuCl_2 \cdot 2\,C_5H_5NO$ shown in Figures 29 and 30, page 35, are similar to those of $CuCl_2 \cdot 1\,C_5H_5NO$; $CuCl_2 \cdot 2C_5H_5NO$ maxima appear at 786 mμ in H_2O, 450 and 875 (very broad) mμ in CH_3CN. The molar absorptivities (Table XIII, page 37) of the $CuCl_2 \cdot 2\,C_5H_5NO$ compound are lower than those observed for $CuCl_2 \cdot 1\,C_5H_5NO$. The band

around 450 mμ has been assigned to both octahedral and tetrahedral Cu(II) species in solution (47). However, the data in Table XVI, page 49, indicate a band in this region is probably characteristic of a tetrahedral rather than an octahedral Cu(II) species. This band has not been observed in strongly coordinating solvents (47). The solution spectral data for $CuCl_2 \cdot 2\,C_5H_5NO$ are inadequate and more extensive investigation is necessary before an absolute assignment of a specific configuration for the Cu(II) in solution can be made. The configuration in solution, as has been previously discussed, is not always indicative of the solid state configuration.

The magnetic moment of the bis-α-pyridone copper(II) complex is 1.8 B.M. It is temperature independent and appears to follow the Curie-Weiss Law. This value is within the range observed for both tetrahedral and octahedral Cu(II) compounds. Therefore, it is not possible to determine from the magnetic data alone the configuration of $CuCl_2 \cdot 2\,C_5H_5NO$.

The composite data are not sufficient to propose a configuration for $CuCl_2 \cdot 2\,C_5H_5NO$ in the solid state. The limits of the reflectance spectrum require extension before this information will be useful. Additional solution spectra in weak coordinating colvents will be necessary before a structure for $CuCl_2 \cdot 2\,C_5H_5$ can be established.

Dichloro-tris-α-pyridone Cobalt(II)

The magnetic moment of this compound is 4.85 B.M. at room temperature and is temperature independent. This value is within the range normally accepted for octahedral spin-free Co(II) compounds. M. Goodgame has

prepared octahedral diiodo-tris-(dipyridylamine) cobalt(II) and reported a magnetic moment of 4.94 B.M. (59). Biagette and Haendler (69) have prepared $Co(NO_3)_2 \cdot 3\,C_5H_5N$ and found its magnetic moment to be 4.60 B.M. This compound has also been assigned an octahedral configuration. Bertrand and Plymale (83) have prepared tetrahedral $CoCl_2 \cdot 3\,C_5H_5NO$ (pyridine-N-oxide) and found its magnetic moment is 4.67 B.M. It appears as though an octahedral structure is favored for the tris-α-pyridone complex, but a tetrahedral structure cannot be ruled out by magnetic data alone.

The diffuse reflectance spectrum shown in Figure 35, page 38, for $CoCl_2 \cdot 3\,C_5H_5NO$ has maxima at 450(sh), 515, 530 and 640 mμ. The octahedral compound prepared by M. Goodgame, mentioned above, has reflectance maxima at 421, 481 and 541 mμ. The octahedral compound prepared by Biagetti and Haendler has reflectance maxima at 480(sh), 530 and 625 mμ. There is also reasonable agreement between the $CoCl_2 \cdot 3\,C_5H_5NO$ data and the data for known octahedral Co(II) compounds presented in Table XIX, page 55, Therefore, $CoCl_2 \cdot 3\,C_5H_5NO$ is probably an octahedral compound.

The solution spectra for $CoCl_2 \cdot 3\,C_5H_5NO$ shown in Figures 31-33, pages 36 and 37, are almost identical to those of $CoCl_2 \cdot 1\,C_5H_5NO$. $CoCl_2 \cdot 3\,C_5H_5NO$ solutions, however, exhibit molar absorptivities closer to the 100 region which is characteristic of octahedral Co(II) species. The lower molar absorptivities, however, do not favor an octahedral Co(II) species when $CoCl_2 \cdot 3\,C_5H_5NO$ is dissolved. Instead, it appears as though both complexes form the same Co(II) species in solution which, on the

basis of the $CoCl_2 \cdot 1\,C_5H_5NO$ solution discussion, supports a tetrahedral Co(II) species in solution.

The reflectance and magnetic data of $CoCl_2 \cdot 3\,C_5H_5NO$ appears to support the conclusion drawn from the x-ray powder data that the two α-pyridone cobalt(II) complexes have different configuration. The data presented for $CoCl_2 \cdot 3\,C_5H_5NO$ suggests the complex is probably octahedral.

SUMMARY

Several new compounds of α-pyridone with the divalent transition metal ions, Mn, Co, Ni and Cu have been prepared by mixing ethanol solutions of anhydrous metal (II) chlorides and α-pyridone. The reaction is represented by the general equation:

$$MCl_2 + n\,C_5H_5NO \xrightarrow{C_2H_5OH} MCl_2 \cdot n\,C_5H_5NO$$

Compounds with n = 1 have been prepared for each of the metal ions used. The compounds precipitate readily upon mixing. The Cu and Co compounds can be recrystallized and purified from C_2H_5OH. The Ni and Mn complexes are less soluble but may also be crystallized from C_2H_5OH. All four compounds have been investigated by x-ray diffraction, magnetic susceptibility, ultraviolet solution spectra, solid and solution visible spectra, infrared spectra and elemental analysis techniques. A projection of single crystal x-ray diffraction data for $CuCl_2 \cdot 1\,C_5H_5NO$ indicates the compound is a chlorine-bridged dimer. The dimers are stacked one on top of the other, giving chains of Cu atoms throughout the structure. The composite data strongly support a distorted tetrahedral structure for $CuCl_2 \cdot 1\,C_5H_5NO$. The unit cells of $CuCl_2 \cdot 1\,C_5H_5NO$ and $CoCl_2 \cdot 1\,C_5H_5NO$ are clearly related and therefore, the Co compound is probably a chlorine-bridged dimer, too. The data obtained also support a distorted tetrahedral structure for $CoCl_2 \cdot 1\,C_5H_5NO$. X-ray powder diffraction data show the Co, Ni and Mn complexes are isomorphic so the Ni and Mn complexes are probably also chlorine-bridged tetrahedral dimers. While not unequivocal, the composite

evidence presented for the Ni and Mn compounds also supports a tetrahedral structure for these two compounds.

A Co compound in which n = 3 has been prepared and investigated in a like manner, but without single crystal x-ray diffraction analysis. X-ray powder diffraction data indicate that this compound is different structurally from the n = 1 Co compound, as would be expected. The data collected and reported appear to favor an octahedral structure for the n = 3 compound.

An n = 2 Cu compound has also been prepared and investigated. The data collected are inadequate to support a specific configuration for this compound.

APPENDIX A

The Attempted Preparation of Bis-acetamido Copper(II)

EXPERIMENTAL PROCEDURES AND RESULTS

Purification of Acetamide

Acetamide used in this study was purified by recrystallization from CH_3OH as outlined by Wagner (84). The product appeared as long white needles which melt at 80.5°C. It was also examined by nitrogen and infrared analysis. Figure 41 represents an infrared spectrum of acetamide. The spectrum is very similar to one published by Kutzelnigg and Mecke (85).

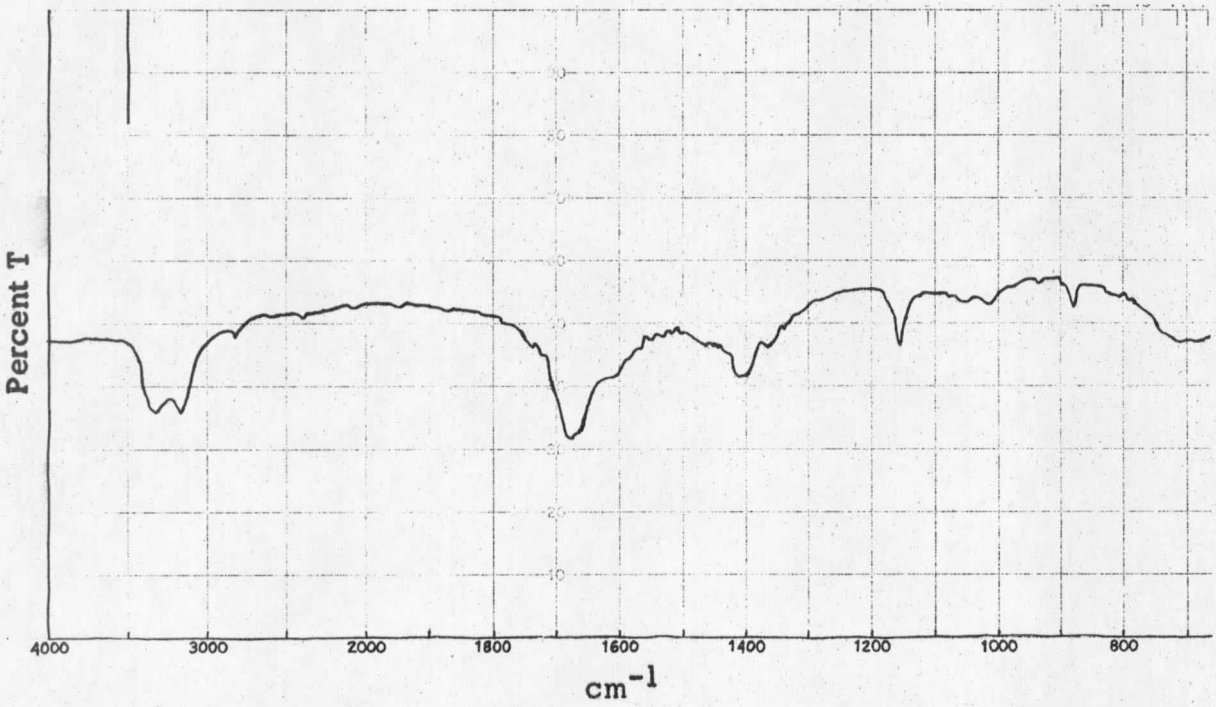

Figure 41. Infrared Spectrum of Acetamide

Nitrogen analyses yield 23.3% nitrogen found against 23.7% nitrogen calculated. The purified product was stored in capped bottles over anhydrous $CaSO_4$.

Preparation and Identification of Sodium Acetamide

Sodium acetamide was prepared by the following reaction scheme:

$$Na + C_2H_5OH \longrightarrow Na^{\oplus}EtO^{\ominus} \xrightarrow{CH_3CONH_2} Na^{\oplus}CH_3CONH^{\ominus} + C_2H_5OH$$

A three-neck round bottom flask was equipped with a reflux condenser, pressure-equalizing dropping funnel and nitrogen gas inlet. The flask was immersed in an ice bath and stirred magnetically. Sodium metal was freshly cut in a glove bag to approximately one cubic centimeter chunks just before use; the chunks were placed in a small single-neck flask fitted with a rubber sleeve that could be closed with a screw clamp. The sodium metal was added to the reaction flask by sliding the sleeve over a joint and inverting the flask containing the sodium metal. The reaction flask was flushed with dry nitrogen for ten minutes before the sodium metal was added. The system was continuously flushed with dry nitrogen during the reaction. Absolute C_2H_5OH, dried by distillation from Mg turnings, was added slowly through the dropping funnel to the sodium metal with stirring. Approximately 300 ml of C_2H_5OH was used per molecular weight of sodium metal. The reaction proceeds very smoothly under these conditions. After disappearance of the sodium metal, the mixture was stirred for one hour without the ice bath. A C_2H_5OH solution of acetamide was then added dropwise to the reaction mixture with stirring. Following final addition of the acetamide, the mixture was warmed to approximately 60°C and stirred for one hour. The C_2H_5OH was then removed by vacuum distillation and the product washed with dry ether and dried in vacuo over KOH for 24 hours. The product is a white

hygroscopic powder. It was stored over KOH or anhydrous $CaSO_4$ in tightly closed bottles.

Figure 42 is an infrared spectrum of sodium acetamide. The spectrum was difficult to obtain because the compound was hygroscopic; it is essentially identical to one published by Kutzelnigg and Mecke (85). Sodium

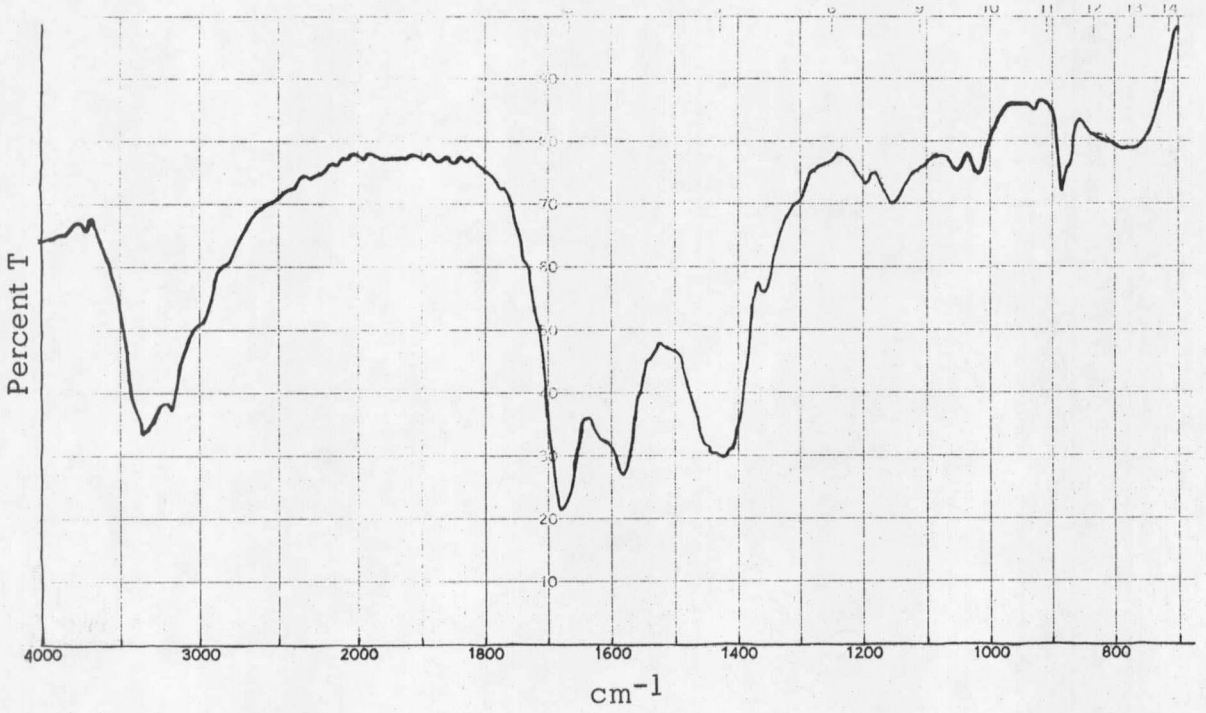

Figure 42. Infrared Spectrum of Sodium Acetamide

acetamide was analyzed for nitrogen content and the base equivalent in water was determined by standard acid titrimetry. Typical results are listed in Table XXII. Solubility characteristics of sodium acetamide were determined by placing 10 mg of sodium acetamide in 1 ml of solvent at room temperature (except for acetamide which was molten); the mixtures stood for

one hour before visual examination was used to determine solubility. The results are shown in Table XXIII.

Table XXII

Sodium Acetamide Analyses

Base Equivalent Determined vs. Standard HCl

Trial	1	2	3
Found	0.963±0.023	0.992±0.007	0.982±0.007
Calc.	1	1	1
% N			
Found		17.7±0.007	16.4±0.29
Calc.		17.3	17.3

Table XXIII

Sodium Acetamide Solubilities

Soluble	Partially Soluble	Insoluble
Acetamide	Dimethyl sulfoxide	Acetone
Amyl Alcohol	Tertiary Butyl Alcohol	Acetonitrile
Ethyl Alcohol		Benzene
Ethylene Glycol		Bis(2-ethoxyethyl)ether
Isopropyl Alcohol		Carbon Tetrachloride
Methyl Alcohol		Chloroform
Pyridine		Diethyl Ether
Water		Dioxane
		Ethyl Acetate
		N,N,Dimethylformamide

Attempted Syntheses of Bisacetamido Copper(II) Complexes

Direct Combination

Copper(II) cation is a strong Lewis acid and the acetamido anion is a strong Lewis base; the reaction:

$$NaCH_3CONH + CuCl_2 \xrightarrow{solvent} NaCl + Cu(CH_3CONH)_2 \cdot l\,solvent$$

was thus attempted under a wide variety of conditions. $NaCH_3CONH$ and anhydrous $CuCl_2$ were dissolved in a common solvent or different solvents. Molar ratios of 1 Cu(II):2 $NaCH_3CONH$ were used throughout. These solutions were mixed in a reaction vessel and stirred. Some solvents gave an immediate precipitate, but others required prolonged stirring and/or heating before precipitation occurred. Some solvents required partial evaporation before solids formed. The solvents listed in Table XXIV were used in the attempted syntheses.

Table XXIV

Solvents Used in Attempted Syntheses

Acetamide	Chloroform	Formamide
Acetic anhydride	Dichloromethane	Glycerol
Acetone	Diethyl ether	Isoamyl alcohol
Acetonitrile	Dimethylsulfoxide	Isobutyl alcohol
Amyl alcohol	Dimethylformamide	Isopropyl alcohol
Benzene	Dioxane	Methyl alcohol
Bis-(2-ethoxyethyl)ether	Ethylacetate	Propyl alcohol
Butyl alcohol	Ethyl alcohol	Pyridine
Carbon tetrachloride	Ethylene glycol	Tertiary butyl alcohol

The solids were separated by filtration and analyzed to determine their composition. Solvents were evaporated from the filtrates by heating and/or vacuum distillation and the resulting residues were analyzed. Table XXV lists the results of selected attempts.

To replace total coincident mixing of the reactant solutions, dropwise addition of one reactant solution to the other was tried in the hope that this

Table XXV

Results of Selected Bisacetamido Copper(II) · 1 Solvent Synthesis

Solvent	Time Required for Pptn.	Nature of Product	% Cu Found	% Cu Calc.[d]	Remarks
Acetone + i-propyl alc.[a]	immediate	green amorphous	11.9	26.8	1)Soluble only in strong acid
Acetone + i-propyl alc.[a]	immediate	green amorphous	46.7	26.8	2)Soluble only in strong acid
Pyridine[b]	immediate	brown amorphous	---	24.5	1)I.R. shows NH present in original ppt; absent in solvent residue
Ethylene Glycol[b]	prolonged stirring	blue gummy	49.1	26.3	1)I.R. shows NH absent in original ppt. 2)Difficult to obtain a workable solid
Acetamide[b]	immediate NH_3 evolution with ppt. formation	brown	---	26.6	1)I.R. shows NH absent in original ppt. 2)Extremely insoluble
Acetamide[b]	immediate	blue-green powder	19.0	26.6	1)I.R. shows NH absent in original residue 2)Turns brown upon standing 3)Original ppt extremely insoluble
Ethanol[b]	immediate	blue powder	---	28.1	1)NaCl evident in product; confirmed by x-ray powder diffraction
		blue powder[c]	62.1	28.1	2)C_2H_5OH wash solution was colorless

[a]Upper solvent for $CuCl_2$, lower solvent fof $NaCH_3CONH$
[b]Common solvent
[c]Original residue washed with C_2H_5OH several times to remove NaCl before analysis
[d]Assuming $Cu(CH_3ONH)_2 \cdot 1$ solvent

variation would slow the reaction and permit greater control of product formation. Precipitation occurred or was induced as previously described. The solids were treated in the same manner with results similar to those listed in Table XXV.

A third general technique was placement of both solid reactants in the reaction vessel followed by solvent addition and stirring. Solvents were chosen to control the reactant concentrations in solution and therefore, control the rate of product formation. The solids obtained were analyzed as before with similar results.

An expected product, NaCl, of the reaction under investigation was obtained on several occasions. Its presence was confirmed by x-ray powder diffraction photographs. The presence of NaCl as an impurity in the amorphous residues would certainly affect the elemental analyses. Removal of NaCl from the residues was attempted by washing the residues with C_2H_5OH. The washings were qualitatively checked for $Cl^{\ominus}$ ($AgNO_3$) and $Na^{\oplus}$ (flame test). After several washings, $Na^{\oplus}$ and $Cl^{\ominus}$ were not detectable. The residues remaining were not $Cu(CH_3CONH)_2 \cdot 1$ solvent as shown in Table XXV.

Soxhlet Extraction Techniques

Nucleophilic substitution is commonly used in many organic syntheses. A nucleophilic reagent (nucleophile) is an electron donor to a central acceptor atom. A strong nucleophile will generally replace a weaker nucleophile. Transition metal complexes also take part in nucleophilic

substitution reactions (86). Ligands vary in electron donating characteristics and considerable work has provided a classification of the coordinating strengths of the most common ligands (86). The acetamido and acetate anions are nucleophiles and Lewis bases. Acetic acid has a pKa = 4.76 in H_2O; 10.32 in ethanol (87). Acetamide has a pKa = 15.1 in H_2O; pKa values in other solvents were not available. These pKa values indicate the acetamido anion is a stronger nucleophile than the acetate anion. Therefore, the reaction:

$$Cu(CH_3COO)_2 + 2\,Na(CH_3CONH) \xrightarrow{\text{solvent}}$$
$$2\,Na(CH_3COO) + Cu(CH_3CONH)_2 \cdot 1\,\text{solvent}$$

was considered as another possible synthetic pathway. $Cu(CH_3COO)_2$ (a binuclear bidentate complex) appeared to be a good complex to use in synthesis of $Cu(CH_3CONH)_2 \cdot 1$ solvent by nucleophilic substitution. Several workers have used soxhlet extraction to prepare transition metal complexes (89) so the technique was used in attempted syntheses of $Cu(CH_3CONH)_2 \cdot 1$ solvent by the reaction just shown. Anydrous $Cu(CH_3COO)_2$ was prepared as described by Graddon (90). Here, too, a variety of solvent systems were investigated. The reactants were alternated between the thimble and solution, but always with the same results: brown amorphous insoluble solids were produced.

Soxhlet extraction offered another means of controlling the contact between the reactants so it was substituted for the previously described techniques. The original reactants, $CuCl_2$ and $Na(CH_3CONH)$, were used as well as acetamide and the Pt blue ingredients (described in next section).

The reactants position and solvents were varied as before. As before, the products obtained were not $Cu(CH_3CONH)_2 \cdot 1$ solvent as shown by analyses. Results were similar to those of earlier attempts.

Internal Hydrolysis

One of the first recorded reactions of a coordinated organic ligand was the hydrolysis of acetonitrile coordinated to platinum(II) (91). Gillard and Wilkinson have recently (92) re-examined this reaction and successfully prepared $Pt(CH_3CONH)_2 \cdot 1\,H_2O$ (Platinum blue). They suggest the platinum blue is formed by the hydrolysis of $Pt(CH_3CN)_2Cl_2$ through the reaction:

$$Pt(CH_3CN)_2Cl_2 + 2\,AgNO_3 + 3\,H_2O \longrightarrow$$

$$Pt(CH_3CONH)_2 \cdot 1\,H_2O + 2\,HNO_3 + 2\,AgCl$$

The filtrate from this reaction was acidic and the pH of the filtrate (3.8) was close to the theoretical value (3.7) expected for the molar quantities of the reactants used. Reaction of platinum blue with KCN gave an orange solution which was repeatedly extracted with ether. Concentration of the dried (Na_2SO_4) ether extract gave white crystals, melting point 32°C, whose infrared spectrum was identical with that of acetamide. Chemical and spectroscopic evidence best fit a polymeric structure involving acetamido bridges, with water molecules probably hydrogen bonded within the crystal. This suggested, therefore, that platinum blue might be a binuclear bidentate complex. The complex is diamagnetic. Platinum blue, as presented here, therefore had some of the characteristics expected for $Cu(CH_3CONH)_2 \cdot 1\,H_2O$.

In view of these characteristics, $Cu(CH_3CN)_2Cl_2$ was substituted for $Pt(CH_3CN)_2Cl_2$ to attempt preparation of $Cu(CH_3CONH)_2 \cdot 1H_2O$ by the reaction just described. $Cu(CH_3CN)_2Cl_2$ was prepared by saturating hot CH_3CN with $CuCl_2$ and then cooling the mixture. $Cu(CH_3CN)_2Cl_2$ precipitated as a yellow-gold solid. The $Cu(CH_3CN)_2Cl_2$ and $AgNO_3$ were introduced in the reaction scheme in solution and as solids in a variety of solvents. In all cases, AgCl formed and was removed by filtration. The filtrates were analyzed before and after solvent evaporation. The filtrates were green to blue-green in color and analyses indicated that $Cu(NO_3)_2$ was the dominant product.

Closed System Attempts

Compounds whose color, crystallinity and analyses encouraged further study generally turned brown after removal from the reaction vessel and/or upon attempted recrystallization. This difficulty suggested that the compounds were reacting with O_2 or H_2O upon exposure to the atmosphere or to traces of H_2O present in the recrystallization solvent. Therefore, a system that was oxygen-free and used anhydrous solvents was considered. The technique previously described for the preparation of sodium acetamide (nitrogen atmosphere, dried solvents) provided such a closed system. This system was used in attempted preparations of $Cu(CH_3CONH)_2 \cdot 1$ solvent by one of these two pathways:

1) $Na + C_2H_5OH \longrightarrow Na^{\oplus}C_2H_5O^{\ominus} \xrightarrow{CH_3CONH_2}$

$C_2H_5OH + Na^{\oplus}CH_3CONH^{\ominus} \xrightarrow{CuCl_2} NaCl + Cu(CH_3CONH)_2 \cdot 1C_2H_5OH$

2) $Na + C_2H_5OH \longrightarrow Na^{\oplus}C_2H_5O^{\ominus} \xrightarrow{CuCl_2}$

$NaCl + Cu(C_2H_5O)_2 \xrightarrow{CH_3CONH_2} Cu(CH_3CONH)_2 \cdot C_2H_5OH$

Products of these reactions were green or blue and amorphous. The solids were separated from the reaction mixture by filtration in a glove bag and dried in vacuo before analysis. Results are listed in Table XXVI with other closed system results.

Table XXVI

Closed System Results

Trial	$Cu(CH_3CONH)_2 \cdot C_2H_5OH$		$Ni(CH_3CONH)_2 \cdot C_2H_5OH$		$Cu(C_6H_5CONH)_2 \cdot C_2H_5OH$	
1	Found 34.8% Cu	1.68%N	1.31% N		25.8% Cu	1.31% N
	Calc. 28.2%	12.4 %	10.5 %		18.2%	8.00%
2	Found 56.6% Cu				29.0% Cu	1.21% N
	Calc. 28.2%	----	----		18.2%	8.02%

Attempted Synthesis of Bisacetamido Nickel(II) Complex

The properties of the Cu(II) products suggested the use of a different transition metal ion to determine if the nature of the metal ion might be a controlling factor in product stability. Basolo and Pearson (86) indicate that Ni(II) complexes are more inert, generally, to nucleophilic attack than Cu(II) complexes. Orgel (93) suggests that octahedral and tetrahedral Ni(II) complexes are more stable than comparable Cu(II) complexes because of greater ligand field stabilization of d^8 metal ions. Therefore, $NiCl_2$ was substituted for $CuCl_2$ in the above reaction scheme to see if

$Ni(CH_3CONH)_2 \cdot C_2H_5OH$ could be prepared. The results were similar to those of Cu(II). Table XXVI includes the nitrogen analysis of the compound recovered.

Attempted Synthesis of Bisbenzamido Copper(II) Complex

Suspected compound decomposition in the previous Cu(II) attempts also suggested the need for a more stable ligand. The aromatic ring was considered capable or providing some stabilization; $Cu(C_6H_5COO)_2 \cdot C_2H_5OH$ is thought to be a binuclear bidentate complex (17, 94). Benzamide was substituted for acetamide in the closed system to see if $Cu(C_6H_5CONH)_2 \cdot 1$ solvent could be produced. Results similar to acetamide were obtained, as shown in Table XXVI.

DISCUSSION

The results shown in Table XXV, page 75, indicate the general nature of the difficulties encountered throughout this portion of the study. The products isolated were blue, green or brown, amorphous, insoluble solids. Elemental analyses of these solids indicated that $Cu(CH_3CONH)_2 \cdot 1$ solvent was not isolated during the study. Table XXVII lists some compounds that might have been isolated as reaction products.

Table XXVII

Suspected Reaction Products

Compound	Nature	% Cu
$Cu(OH)_2$	blue, amorphous powder	65.5%
$CuCl_2$	tan, amorphous powder	47.0%
$CuCl_2 \cdot 4$ solvent[a]	?	~17.0%
$CuCl_2 \cdot 2\, C_5H_5N$	blue-green crystals	21.6%
$Cu(NO_3)_2 \cdot 3\, H_2O$	blue powder	21.0%
$Cu(CH_3CONH)_2 \cdot 2$ solvent[a]	?	~21.5%
$Cu(CH_3CONH)_2 \cdot 3$ solvent[a]	?	~18.0%
$Cu(CH_3CONH)_2 \cdot 4$ solvent[a]	?	~15.0
$Cu(CH_3COO)_2 \cdot 1\, H_2O$	blue-green crystals	31.6%

[a]acetone, isopropyl alcohol, ethylene glycol, acetamide

The insolubility of the compounds in common non-polar solvents was somewhat unexpected. It seemed reasonable to assume that substitution of a nitrogen atom for an oxygen atom in the ligand would not drastically change the solubility of any products obtained. However, if the acetamido anion was considered a stronger base than the acetate anion, then the bond formed between Cu(II) and the acetamido anion would be more polar and the

the compound would then be less soluble in non-polar solvents. Formation of polymeric compounds might also be a reason for decreased solubility, $CuCl_2$ is a polymeric chain as shown in Figure 43. The chains are infinite

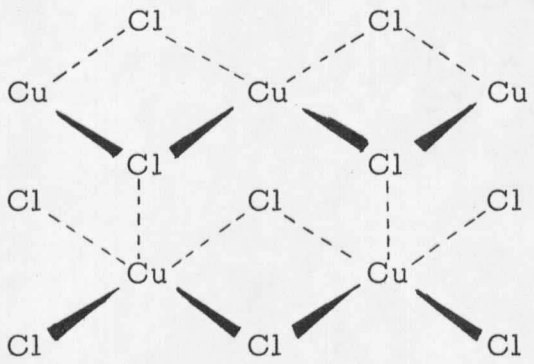

Figure 43. $CuCl_2$ Structure

and the copper atoms show square 4-coordination and have as nearest neighbors, in adjacent chains, two chlorine atoms (45). It might be possible for the acetamido group to form bridges between the chains of $CuCl_2$ and form a less soluble polymer; $CuCl_2$ is soluble in C_2H_5OH. The data collected during the study were insufficient to identify most of the reaction products. A few were identified and will be discussed.

When alcohols were used in the reaction scheme, the products were soluble only in strong acid. This suggested a basic copper(II) compound was produced. This reaction:

$$2\,CH_3CONH^{\ominus} + 2\,H_2O \longrightarrow 2\,CH_3CONH_2 + 2\,OH^{\ominus} \xrightarrow{Cu(II)} Cu(OH)_2$$

could occur if the solvent has not been sufficiently dried. Some of the reaction products darkened during recrystallization and purification attempts

which, again, suggested $Cu(OH)_2$ because it decomposes to give CuO, a black powder (45). X-ray powder diffraction photographs indicated that CuO was present in some of the isolated products.

Reaction systems using pyridine generally produced blue-green needle like crystals from the filtrate; a brown residue formed immediately upon mixing. The blue-green crystals could be recrystallized from pyridine. Visible solution spectra of the recrystallized product gave a normal copper absorption band in the 750 mμ region, but did not have the absorption band attributed to dimeric Cu(II) compounds around 375 mμ(1). Figure 44 is a visible spectrum of the blue-green crystals.

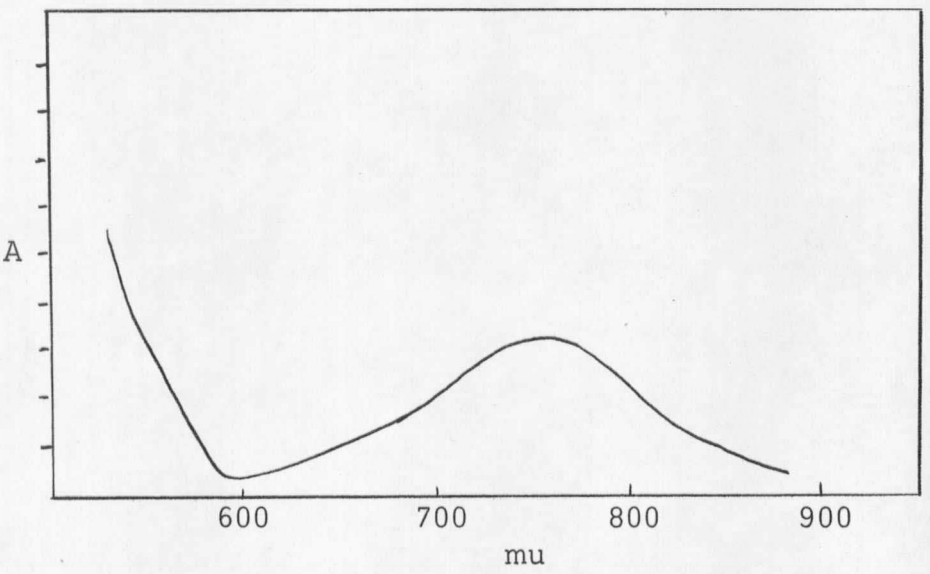

Figure 44. Visible Absorption Spectrum of Blue-Green Crystals from $CuCl_2 \cdot NaCH_3CONH \cdot C_5H_5N$ System

The infrared spectrum (Figure 45), however, clearly indicated that acetamide was not present in the crystals. The copper content of the crystals

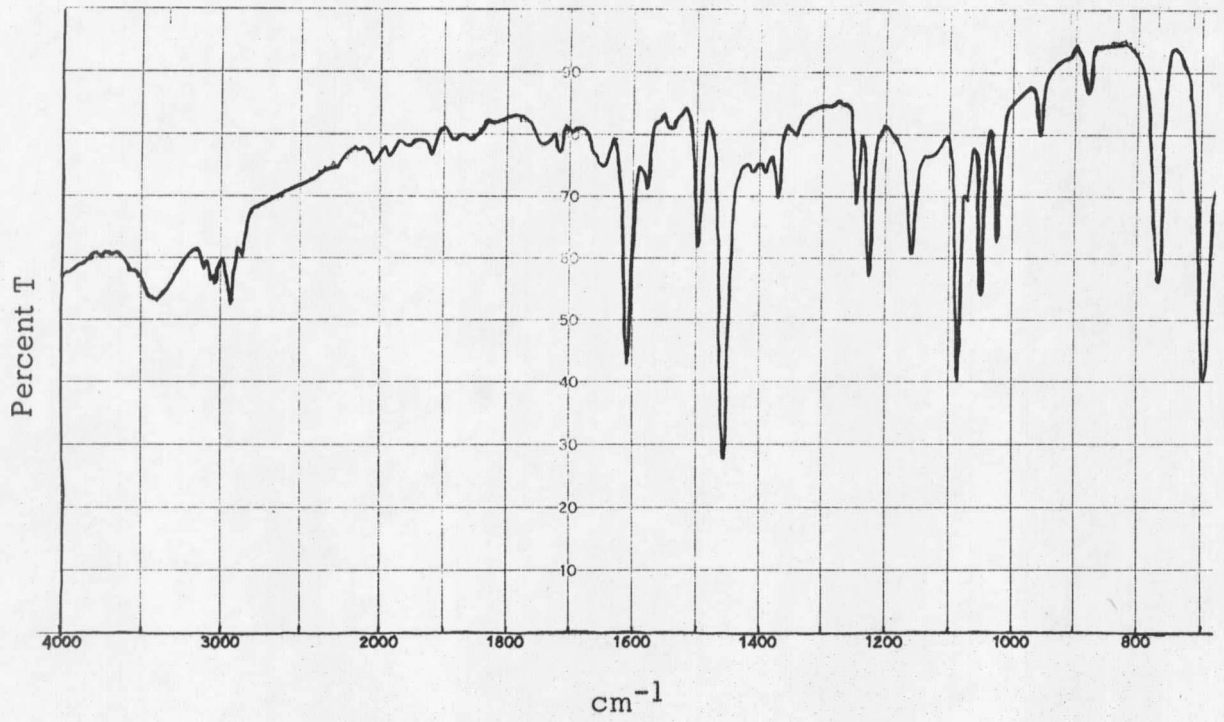

Figure 45. Infrared Spectrum of Blue-Green Crystals from $CuCl_2 \cdot NaCH_3CONH \cdot C_5H_5N$ System

approached that of $CuCl_2 \cdot 2\,C_5H_5N$ (Table XXVI). Therefore, further investigation to identify the blue-green crystals was undertaken. Hot pyridine was almost saturated with $CuCl_2$ and allowed to cool; blue-green needle-like crystals precipitated. These crystals were compared (infrared spectra and x-ray powder diffraction photographs) with the blue-green crystals previously obtained; spectra and photographs for both sets of crystals were identical. Figure 46 is the infrared spectrum of the crystals prepared from $CuCl_2$ and C_5H_5N alone; Figure 47 is an infrared spectrum of pyridine.

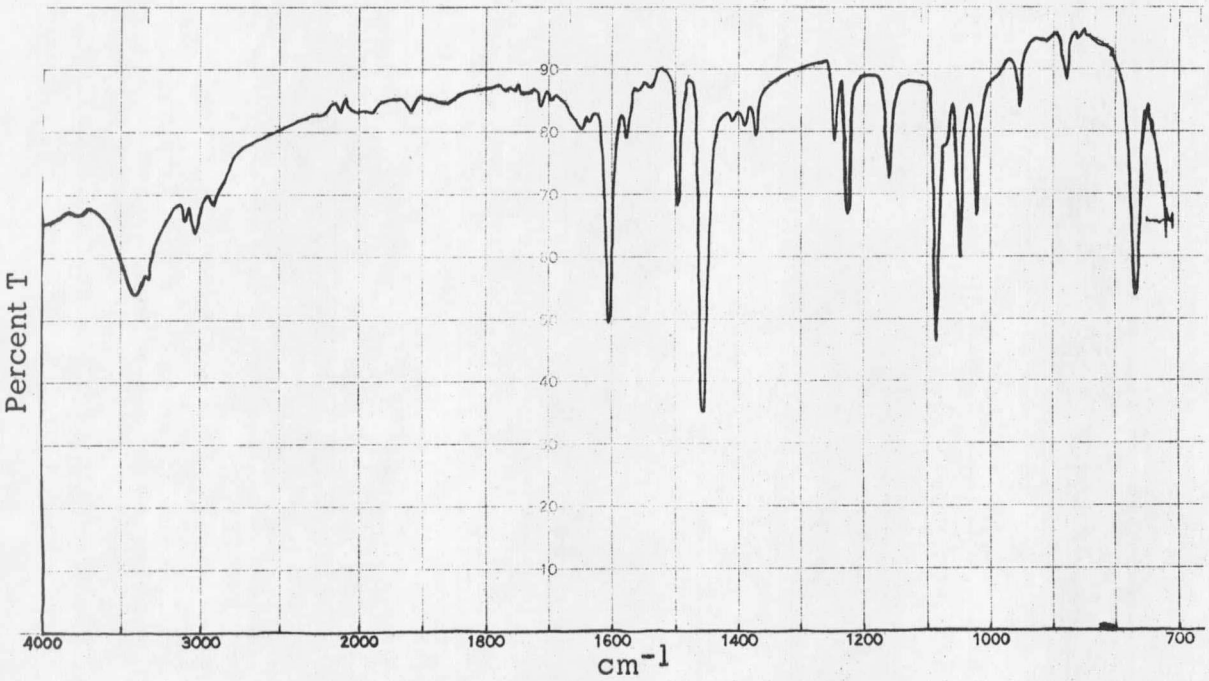

Figure 46. Infrared Spectrum of Blue-Green Crystals from $CuCl_2 \cdot C_5H_5N$ System

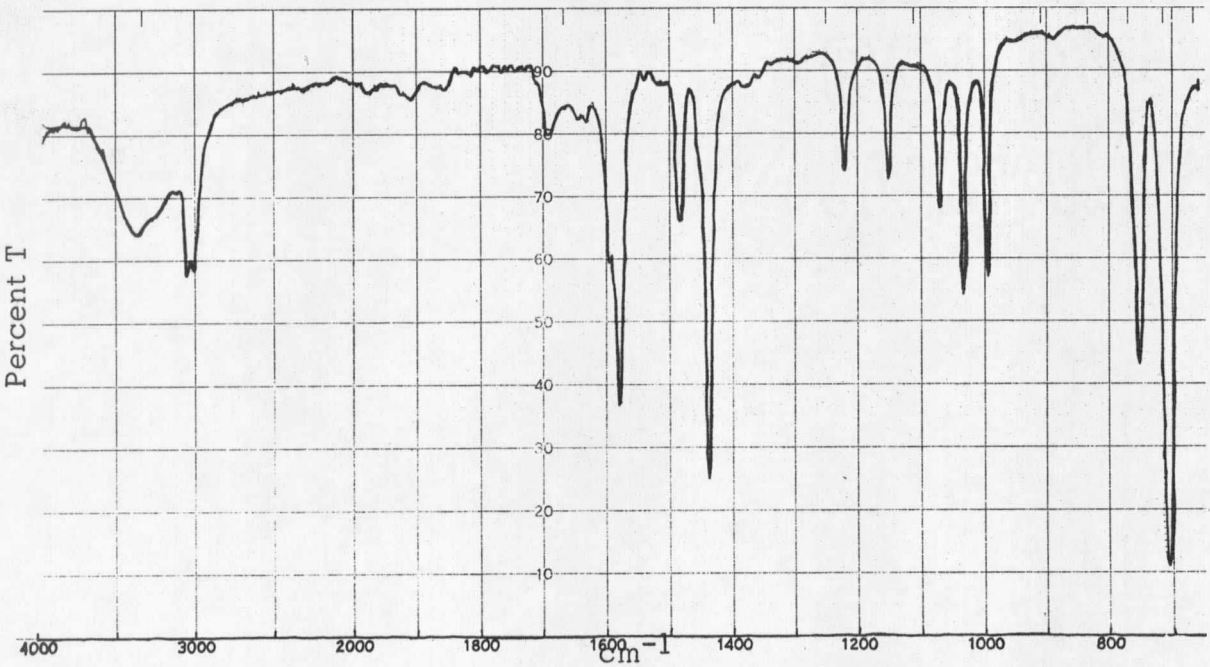

Figure 47. Infrared Spectrum of Pyridine

The infrared spectrum of the original brown residue indicated the presence of sodium acetamide, but insufficient data were gathered to permit absolute identification.

Acetamide has been used as a non-aqueous solvent by Jander and others (88, 95, 96). It is known to undergo autoprotolysis when molten:

$$2\,CH_3CONH_2 \rightleftharpoons CH_3CONH^{\ominus} + CH_3CONH_3^{\oplus}$$

Amides are readily hydrolyzed under either acidic or basic conditions. Nucleophilic attack of the amide occurs with reasonable ease through this type reaction (97):

$$R-C(=O)-NH_2 \xrightarrow{OH^{\ominus}} R-C(O^{\ominus})(OH)-NH_2 \longrightarrow RCOO^{\ominus} + NH_3\uparrow$$

When molten acetamide was used as the solvent in this study, ammonia gas was detected on a number of occasions: this meant acetamide was being hydrolyzed. Molten acetamide itself released no noticeable ammonia; the gas formed when solid sodium acetamide was added to the molten acetamide. The following equations might represent a pathway for producing NH_3 from the reactants.

a) $2\,CH_3CONH_2 \rightleftharpoons CH_3CONH^{\ominus} + CH_3CONH_3^{\oplus}$

b) $CH_3CONH_3^{\oplus} \xrightarrow{Na^{\oplus}CH_3CONH^{\ominus}} (CH_3CO)_2NH + NH_3$

Reaction b) may proceed one step further according to Gruttner (95):

$$(CH_3CO)_2NH + NaCH_3CONH \longrightarrow (CH_3CO)_2N^{\ominus}Na^{\oplus} + CH_3CONH_2$$

Jander and Winkler (88) have used molten acetamide as a solvent for conductometric titrations of heavy metal acetamide complexes with sodium

acetamide. They claim formation of $Cu(CH_3CONH)_2$ and $Na_2[Cu(CH_3CONH)_4]$ when titrating $CuCl_2$ with sodium acetamide in molten acetamide. The compounds were not isolated and analyzed. They show that the color of the reaction mixture changes from green $\longrightarrow$ blue-green $\longrightarrow$ black $\longrightarrow$ dark green $\longrightarrow$ yellow $\longrightarrow$ light yellow, as the molar ratio of $Cu(II):NaCH_3CONH$ increases from 1:0 $\longrightarrow$ 1.4. They do not indicate at what molar concentration of sodium acetamide the colors change or if the change is abrupt or gradual. No mention was made of ammonia gas release during the reaction. The concentration of sodium acetamide in the molten acetamide was only 0.03 N, therefore suggesting the $CH_3CONH^{\ominus}$ concentration was dilute enough to prevent noticeable release of ammonia which might be a driving force of reaction b). Dilute solutions might permit reaction between Cu(II) and $CH_3CONH^{\ominus}$ and prevent formation of $(CH_3CO)_2N^{\ominus}Na^{\oplus}$. During the present study, sodium acetamide and $CuCl_2$ concentrations were greater than 0.1 N; NH_3 was detected, which suggested the $CH_3CONH^{\ominus}$ was consumed in the production of NH_3 and $(CH_3CO)_2N^{\ominus}Na^{\oplus}$. The products of the reaction, therefore, might be $Cu[(CH_3CO)_2N]_2$ or $Na_2Cu[(CH_3CO)_2N]_2Cl_2$. The latter compound contains 16.5% Cu and would not exhibit an N-H absorption in an infrared spectrum. This compound might be blue-green, which suggested that the blue-green powder obtained from the second reported molten acetamide reaction (Table XXV, page 75) might be $Na_2Cu[(CH_3CO)_2N]_2Cl_2$. However, insufficient data prevented more definite identification.

The results of this portion of the study clearly indicated that synthesis and isolation of copper(II) acetamide was more difficult than initially anticipated. Variation of solvents and mixing techniques did not change the results. Attempts to increase product stability resulted in similar difficulties.

Why isolation of $Cu(CH_3CONH)_2 \cdot 1$ solvent was not accomplished remains an unsolved problem and deserves additional investigation. This study has evoked the following suggestions for further investigation:

1. Use dilute reactant concentrations ($CuCl_2$ and $NaCH_3CONH$) with molten acetamide to see if the compounds claimed by Jander and Winkler can be isolated and identified; consider the possibilities of double salt formation.
2. An investigation of the reaction between molten acetamide and sodium acetamide; isolation and identification of reaction products. Study the kinetics of the reaction to determine if NH_3 solubility, $CH_3CONH^{\ominus}$ concentration of $Na^{\oplus}$ concentration are controlling factors.
3. Performance of the reaction under vacuum conditions.
4. Introduce gas chromatographic and mass spectroscopic analytical techniques to aid identification of isolated products.
5. Initiate study to determine if the asymmetry of the acetamide group (C-N = 1.33 Å, C-O = 1.26 Å) might prevent syn-syn bidentate binuclear coordination.
6. Synthesis and investigation of transition metal compounds with substituted amides.

LITERATURE CITED

1. M. Kato, H. B. Jonassen and J. C. Fanning, Chem Rev. 64, 99 (1964).
2. J. G. Ross and Y. Yates, Trans. Faraday Soc., 55, 1064 (1959).
3. Ibid. p. 1057.
4. D. J. Royer, Inorg. Chem., 4, 1830 (1965).
5. L. S. Forster and C. J. Ballhausen, Acta Chem. Scand., 16, 1385 (1962).
6. A. W. Schluetter, R. A. Jacobson and R. C. Rundle, Inorg. Chem., 5, 227 (1966).
7. G. F. Kokoszka, H. C. Allen and G. Gordon, J. Chem. Phys., 42, 3693 (1965).
8. C. W. Reimann, G. F. Kokoszaka and G. Gordon, Inorg. Chem., 4, 1082 (1965).
9. A. E. Hansen and C. J. Ballhausen, Trans. Faraday Soc., 61, 631 (1965).
10. W. E. Hatfield and J. S. Paschal, J. Am. Chem. Soc., 86, 3888 (1964).
11. H. L. Schaefer, J. C. Morrow and H. M. Smith, J. Chem. Phys., 42 504 (1965).
12. Y. Muto and H. B. Jonassen, Bull. Chem. Soc. Japan, 39, 58 (1966).
13. J. N. van Niekirk and F. R. L. Schoening, Acta Cryst., 6, 227 (1953).
14. R. Chidambaram and G. M. Brown, A.C.A. Meeting Abstracts, Gatlinburg, Tenn., 1965.
15. D. P. Graddon, J. Inorg. Nucl. Chem., 11, 337 (1959).
16. M. Kishita, M. Inone and M. Kubo, Inorg. Chem., 3, 237 (1964).
17. R. D. Gillard, D. M. Harris and G. Wilkinson, J. Chem. Soc., 2838 (1964).
18. R. Kiriyama, H. Ibamoto and K. Matsuo, Acta Cryst., 7, 482 (1954).
19. G. A. Barclay and R. L. Kennard, J. Chem. Soc., 3289 (1961).
20. Ibid, p. 5244.

21. J. N. van Niekirk and F. R. L. Schoening, Acta Cryst., 6, 501 (1953).

22. R. L. Martin and H. Waterman, J. Chem. Soc., 1359 (1959).

23. G. A. Barclay, et al, Proc. Chem. Soc., 264 (1961).

24. I. M. Kolthoff and E. B. Sandell, Textbook of Quantitative Inorganic Analysis, 3rd Edition, Macmillan Co., N. Y., N. Y., 1952.

25. F. J. Welcher, The Analytical Use of Ethylenediaminetetracetic Acid, D. van Nostrand Co., Inc., Princeton, N. J., 1958.

26. B. N. Figgis and R. S. Nyholm, J. Chem. Soc., 4190 (1958).

27. M. J. Buerger, Crystal Structure Analysis, John Wiley and Sons, Inc., N. Y., N. Y., 1960.

28. A. R. Pray, Inorganic Syntheses, Vol. V, Therald Moeller, Editor-in-Chief, McGraw-Hill Book Co., N. Y., N. Y., 1957.

29. J. V. Quagliano, et al. J. Am. Chem. Soc., 83, 3770 (1961).

30. A. R. Katritsky, Editor-in-Chief, Physical Methods in Heterocyclic Chemistry, Vol. II, Academic Press, N. Y., N. Y., 1963.

31. S. F. Mason, J. Chem. Soc., 4874 (1957).

32. J. A. Gibson, W. Kynaston, A. S. Lindsey, J. Chem. Soc., 4340 (1955).

33. Y. N. Scheinker and N. M. Reznikov, Doklady Akad. Nauk. S. S. R., 102 109 (1955).

34. K. Hoegerle and H. Erlenmeyer, Helv. Chim. Acta, 39, 1203 (1956).

35. A. Albert and E. Spinner, J. Chem. Soc., 1221 (1960).

36. E. Spinner, ibid., p. 1226.

37. L. J. Bellamy and P. E. Rogasch, Proc. Royal Soc., A257, 98 (1960).

38. C. L. Bell, J. P. Shaffner and L. Bauer, Chem. and Ind., 1353 (1963).

39. B. R. Penfold, Acta Cryst., 6, 591 (1953).

40. S. F. Mason, J. Chem. Soc., 5010 (1957).

41. B. N. Figgis and C. M. Harris, J. Chem. Soc., 855 (1959).

42. A. W. Schluetter, R. A. Jacobson, and R. E. Rundle, Inorg. Chem., 5, 277 (1966).

43. M. Bukorska and M. A. Porai-Koshits, Kristallografiya, 5, 127 (1960).

44. W. E. Hatfield and T. S. Piper, Inorg. Chem., 3, 841 (1964).

45. R. B. Heslop and P. L. Robinson, Inorganic Chemistry, Elsevier Pub. Co., Amsterdam, 1960.

46. A. F. Wells, J. Chem. Soc., 1670 (1947).

47. R. A. Howald, private communication.

48. Leo Allen Bares, Thesis (M.S.) Montana State University, December, 1965.

49. L. H. Helmholz and R. F. Kruh, J. Am. Chem. Soc., 74, 1176 (1952).

50. W. R. McWhinnie, J. Chem. Soc., 2959 (1964).

51. P. Ros and G. C. A. Schmit, Theo. Chim. Acta, 4, 1 (1966).

52. D. P. Graddon, J. Inorg. Nucl. Chem., 17, 222 (1961).

53. H. B. Jonassen and A. Weissberger, Editors, Techniques of Inorganic Chemistry, Vol. IV, Interscience Publishers, N. Y., N. Y., 1965.

54. N. S. Gill and R. S. Nyholm, J. Chem. Soc., 4000 (1959).

55. G. J. Janz and A. E. Marcinkowsky, U.S.A.E.C., NYO-8525, 190 pp., (1961).

56. H. C. A. King, E. Körös and S. M. Nelson, J. Chem. Soc., 5449 (1963).

57. F. A. Cotton, D. M. L. Goodgame and M. Goodgame, J. Am. Chem. Soc., 83, 4690 (1961).

58. H. N. Ramaswamy and H. B. Jonassen, Inorg. Chem., 4, 1595 (1965).

59. M. Goodgame, J. Chem. Soc., A-1, 63 (1966).

60. W. Libus and I. Uruska, Inorg. Chem., 5, 256 (1966).

61. D. A. Fine, J. Am. Chem. Soc., 84, 1139 (1962).

62. I. I. Antipova-Karataeva and E. E. Vainshtein, Fiz. Probl. Spektroskopii, Adal. Nauk. S. S. R., Meterialy 13-go Trinadtsatogo Sovesch, Leningrad, 1960, 1, 339 (1962).

63. R. F. Pasternack and R. A. Plane, Inorg. Chem., 4, 1171 (1965)

64. C. J. Ballhausen and Chr. K. Jørgensen, Acta Chem. Scand., 9, 397 (1955).

65. J. Ferguson, J. Chem. Phys., 32, 533 (1960).

66. H. A. Øye and D. M. Gruen, Inorg. Chem., 4, 1173 (1965).

67. J. Ferguson, J. Chem. Phys., 39, 116 (1963).

68. A. B. P. Lever, Inorg. Chem., 4, 763 (1965).

69. R. V. Biagetti and H. M. Haendler, Inorg. Chem., 5, 383 (1966).

70. S. M. Nelson and T. M. Shepherd, J. Chem. Soc., 3276 (1965).

71. M. Ciampolini and N. Nardi, Inorg. Chem., 5, 41 (1966).

72. R. S. Drago, J. T. Donaghue and D. W. Herlocker, Inorg. Chem., 4, 836 (1965).

73. D. M. L. Goodgame and M. Goodgame, J. Chem. Soc., 207 (1963).

74. C. R. C. Coussmaker, et al, J. Chem. Soc., 2705 (1961).

75. D. W. Meek, R. S. Drago and T. S. Piper, Inorg. Chem., 1, 285 (1962).

76. M. Dennis Glonek, C. Curran and J. V. Quagliano, J. Am. Chem. Soc., 84, 2014 (1962).

77. M. C. Browning, et al, J. Chem. Soc., 693 (1962).

78. J. R. Allen, et al, J. Inorg. Nucl. Chem., 27, 1529 (1965).

79. M. Ciampolini and G. P. Speroni, Inorg. Chem., 5, 45 (1966).

80. F. A. Cotton, D. M. L. Goodgame and M. Goodgame, J. Am. Chem. Soc., 84, 167 (1962).

81. C. Furlani and A. Furlani, J. Inorg. Nucl. Chem., 19, 51 (1961).

82. J. R. Allen, et al, J. Inorg. Nucl. Chem., 27, 1865 (1965).

83. J. A. Bertrand and D L. Plymale, Inorg. Chem., 3, 775 (1964).

84. E. C. Wagner, J. Chem. Ed., 7, 1135 (1930).

85. W. Kutzelnigg and R. Mecke, Spectrochim. Acta, 18, 549 (1962).

86. F. Basolo and R. G. Pearson, Mechanisms of Inorganic Reactions, John Wiley and Sons, Inc , N. Y., N. Y., 1958.

87. H. A. Laitinen, Chemical Analysis, McGraw-Hill Book Co., Inc., N. Y., N. Y., 1960.

88. G. Jander and H. Spandau, Chemistry in Non-aqueous Solvents, Vol. 4, G. Winkler, Editor-in-Chief, John Wiley and Sons, Inc., N. Y., N. Y., 1963.

89. H. B. Jonassen, private communication.

90. D. P. Graddon, J. Inorg. Nucl. Chem., 17, 222 (1961).

91. K. A. Hofmann and G. Bugge, Ber., 41, 312 (1908).

92. R. D. Gillard and G. Wilkinson, J. Chem. Soc., 2835 (1964).

93. L. E. Orgel, An Introduction to Transition Metal Chemistry . . . Ligand Field Theory, Methuen and Co., Ltd., London, 1960.

94. J. Lewis and F. Mabs, J. Chem. Soc., 3894 (1965).

95. B. Grüttner, Zeit. Anorg. Chemie, 270, 233 (1952).

96. L. F. Yostema and L. F. Audrieth, J. Am. Chem. Soc., 52, 2693 (1930).

97. R. T. Morrison and R. N. Boyd, Organic Chemistry, Allyn and Bacon, Inc., Boston, 1959.